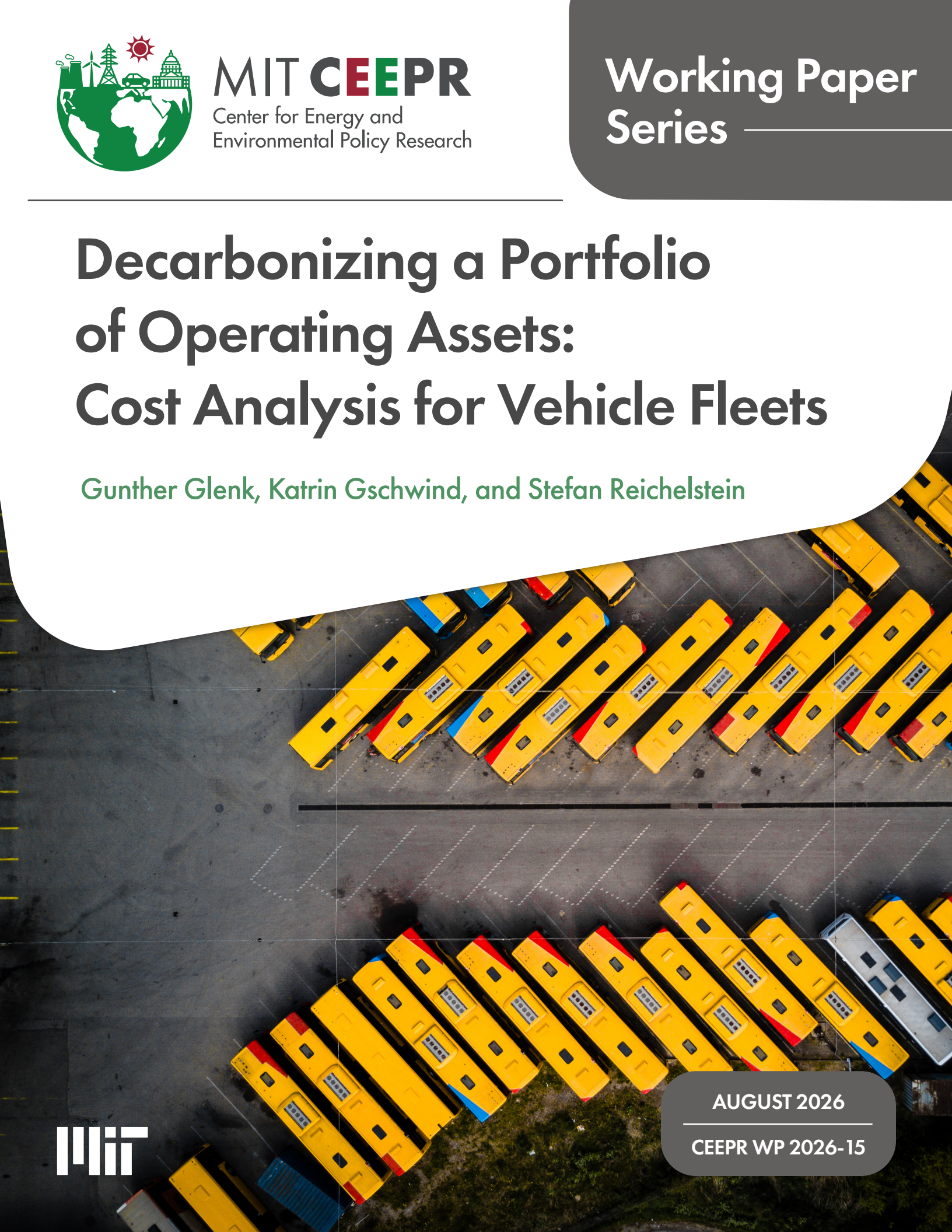
MIT CEEPR
Center for Energy and Environmental Policy Research

Working Paper Series

Decarbonizing a Portfolio of Operating Assets: Cost Analysis for Vehicle Fleets

Gunther Glenk, Katrin Gschwind, and Stefan Reichelstein



AUGUST 2026

CEEPR WP 2026-15

Working Paper Series.

Since 1977, the Center for Energy and Environmental Policy Research (CEEPR) has been a focal point for research on energy and environmental policy at MIT. CEEPR promotes rigorous, objective research for improved decision making in government and the private sector, and secures the relevance of its work through close cooperation with industry partners from around the globe. Drawing on the unparalleled resources available at MIT, affiliated faculty and research staff as well as international research associates contribute to the empirical study of a wide range of policy issues related to energy supply, energy demand, and the environment.

An important dissemination channel for these research efforts is the MIT CEEPR Working Paper series. CEEPR releases Working Papers written by researchers from MIT and other academic institutions in order to enable timely consideration and reaction to energy and environmental policy research, but does not conduct a selection process or peer review prior to posting. CEEPR's posting of a Working Paper, therefore, does not constitute an endorsement of the accuracy or merit of the Working Paper. If you have questions about a particular Working Paper, please contact the authors or their home institutions.

Decarbonizing a Portfolio of Operating Assets: Cost Analysis for Vehicle Fleets

Gunther Glenk*
Business School, University of Mannheim
glenk@uni-mannheim.de

Katrin Gschwind*
Business School, University of Mannheim
katrin.gschwind@uni-mannheim.de

Stefan Reichelstein
Business School, University of Mannheim
Leibniz Centre for European Economic Research (ZEW)
Graduate School of Business, Stanford University
reichelstein@uni-mannheim.de

June 2026

*We thank Scott Arjun, Jan Böckmann, Yunus Keskin, Thomas Kourouxous, Sebastian Menges, Clemens Thielen, and colleagues at the University of Mannheim for their valuable suggestions and discussions. We are particularly grateful to Yuna Haas, Vitus Lüntzel, and Carolin Schiefer for their collaboration in data collection, and to Sina Hafner for writing her graduate thesis on a related topic. We also thank Vivien Haendly, Viviana von den Driesch, and Carolin Witzel for excellent research assistance. Financial support for this study was provided by the Federal Ministry for Economic Affairs and Energy of Germany, the German Research Foundation (DFG Project-ID 403041268, TRR 266), and the Ministry for the Environment, Climate and Energy Sector of Baden-Württemberg.

Abstract

Companies across industries seek to assess the costs of complying with environmental regulations and meeting voluntary emission targets. This paper develops a carbon abatement cost model for firms operating a portfolio of assets with differing cost or load profiles. The resulting abatement cost curves serve as a decision tool for configuring individual assets to achieve firm-wide emission reductions at least cost. We apply our model to urban bus fleets regulated under the California Cap-and-Trade Program. We find that a carbon price of $35 per ton of CO_2e (2024 average) incentivizes firms to configure their fleets such that battery-electric drivetrains constitute 70% of usable installed capacity and 92% of annual demand, while diesel drivetrains serve peak loads. Since the resulting emissions are fairly inelastic to the carbon price, we conclude that the life-cycle cost per mile would increase substantially if deep decarbonization were to be induced entirely by higher carbon prices.

Keywords: life-cycle costing, capacity investments, abatement cost curves, carbon emissions, transport decarbonization

JEL Codes: M41, M48, Q54, Q56

1 Introduction

Companies in multiple industries face the challenge of assessing the costs of meeting voluntary carbon emission targets or complying with environmental regulations. For firms relying on a portfolio of operating assets, the decarbonization task is to optimize targeted changes for individual assets that differ in their cost or load profiles. Salient examples of such asset portfolios are commercial vehicle fleets, such as taxis, buses, trucks, cargo ships, and airplanes.[1] Similar to firms in other industries, fleet operators seek to assess the economics of new drivetrain technologies across vehicles with varying duty cycles to achieve targeted emission reductions for the entire fleet.

This paper develops an abatement cost model for a portfolio of operating assets. Our base model considers a firm that acquires a vehicle fleet to meet a given, time-variant energy demand for transportation services. Each vehicle can be equipped with up to two drivetrain technologies, such as battery-electric and diesel, with combinations reflecting plug-in hybrid vehicles. The *Total Cost of Ownership* (TCO) of the fleet comprises all capacity-related and operational costs associated with the initial configuration and subsequent utilization of each vehicle, consistent with the notion of life-cycle costing in the accounting literature (Labro, 2019; Horngren et al., 2015; Atkinson et al., 2020). Minimizing this life-cycle cost metric yields a closed-form solution for identifying the cost-efficient capacity sizes and deployment of drivetrains for each vehicle. Specifically, the configuration is determined by the point at which a vehicle's *load duration curve*, the ordered demand profile it must satisfy, crosses a capacity utilization threshold given by its cost profile.

We calibrate our model framework to urban bus fleets in the current economic environment of California. Urban buses are heavy-duty vehicles that contribute to both global carbon emissions and local air pollution. Public transit agencies have also been among the first fleet operators to adopt low-emission drivetrain technologies (BNEF, 2025). Based on new industry data for a fleet of 50 vehicles, our calculations project that the cost-efficient fleet comprises 41 plug-in hybrid, nine diesel, and no fully electric buses. Across vehicles in the fleet, electric drivetrains constitute 66% of usable installed capacity and deliver 88% of annual demand. Diesel drivetrains effectively function as "peaker" capacity, covering mainly occasional days of high demand.

[1] Transportation contributes about 15% of global annual greenhouse gas emissions (IPCC, 2023), with a large share stemming from commercial vehicle fleets. Jurisdictions worldwide have therefore enacted targeted policies, including vehicle registration bans, performance standards, and emission charges.

We embed the TCO framework in a context where the fleet operator is tasked with meeting a particular direct (Scope 1) emission target. Such targets may stem from voluntary climate pledges or regulatory mandates such as registration bans or performance standards. For alternative targets, the *Total Abatement Cost* (TAC) is given by the total cost of ownership of the fleet that is minimal among all fleets whose future annual emissions do not exceed the target level. This cost measure yields a simple selection rule that decentralizes the challenge of decarbonizing the fleet to individual vehicles by supplementing the capacity utilization threshold in the unconstrained closed-form solution with the shadow price of meeting the fleet-wide emission target.

Our calculations for urban bus fleets show that their total abatement cost curves are strictly convex in abatement targets, reflecting the shape and relative distribution of load duration curves across vehicles. In particular, firms can achieve initial emission reductions at relatively low cost by expanding the electric capacity of plug-in hybrid buses with low initial electrification. Yet, total abatement costs rise sharply as firms pursue more ambitious targets and must electrify diesel buses, though this additional electric capacity will be used rarely and thus yields limited emission reductions. Despite the sharp increase in total abatement costs, our calculations project that even the lowest technologically feasible emission target increases the total cost of ownership by only 2.6% relative to the cost-efficient fleet.

We then examine the incentives for firms to adopt electric drivetrains in response to emission charges. These charges may reflect a carbon tax or market prices for emission permits under a cap-and-trade system, such as the California Cap-and-Trade Program. We find that if firms in California were to expect prevailing carbon prices to remain at their 2024 average value of \$35 per ton of carbon dioxide equivalent (CO_2e), they would be incentivized to expand electric drivetrains across vehicles such that they constitute 70% of usable installed capacity and 92% of annual demand. This reduces annual direct emissions by 31% relative to the cost-efficient fleet. At the same time, we find that the optimal emission response to carbon prices is highly inelastic due to convex tails of the load duration curves of the buses.[2] If deep decarbonization of urban bus fleets is to be induced by carbon prices, these prices would thus have to rise to several hundred dollars per ton of CO_2e.

A recurring concern in the public debate on carbon regulation is how alternative policy

[2]Recent empirical research in environmental economics finds that transport emissions respond only modestly to carbon prices, partly due to slow fleet turnover (Jacobsen and van Benthem, 2015; Timmins et al., 2009). Our analysis shows that this elasticity also depends strongly on the routes fleet vehicles are to serve.

instruments affect the production costs of essential goods and services. Our cost framework estimates the increase in the levelized cost per mile when deep decarbonization is driven by either mandated emission targets or higher carbon prices.[3] Specifically, if carbon prices in California were to remain at their 2024 average of $35 per ton of CO_2e but urban bus fleets were mandated to reduce direct emissions to the lowest feasible level, their levelized cost per mile would rise by 2.4% relative to no mandate. If the same emission level were to be induced via higher carbon prices instead, the levelized cost per mile would rise by 19.9% relative to no higher carbon prices. This substantially larger increase in private compliance cost reflects higher charges on residual emissions and the fairly inelastic emission response to carbon prices.

Our analysis provides a fairly robust assessment of the cost-efficient configuration and the costs of decarbonizing urban bus fleets today. Yet, rapid advances in battery technology and emerging low-emission fuel substitutes point to further cost reductions in the near term. For example, if battery technology improves as projected (Link et al., 2024), we estimate that (near) complete decarbonization would raise the total cost of ownership by only 1.7–2.4% relative to the cost-efficient fleet. Since the optimal emission response to carbon prices remains fairly inelastic, our results support the view that carbon pricing and emission performance standards are complementary policy instruments for deeply decarbonizing vehicle fleets (Stechemesser et al., 2024). Overall, our findings are consistent with the recent surge in the adoption of battery-electric transit buses worldwide (IEA, 2025b).

Beyond urban buses, our model is directly applicable to other vehicle fleets. Our results indicate that fleets with regular duty cycles anchored at central depots (e.g., delivery vans and trucks, municipal and (air)port vehicles, and local ferries) are prone to high shares of electric drivetrain capacity in the cost-efficient configuration and to achieve deep decarbonization at modest cost. In contrast, fleets operating multi-leg rotations with energy-intensive routes (e.g., long-haul trucks, cargo ships, and commercial airplanes) will likely continue to rely primarily on conventional drivetrains for the cost-efficient configuration in the near future. Moving further afield, we argue that our model can also be adapted to other industries with multiple operating assets. For example, technology companies can adapt our model to assess the costs of deploying renewable energy and storage across data centers worldwide,

[3]Our measure of levelized cost per mile draws on the concept of levelized product costs (Reichelstein and Rohlfing-Bastian, 2015) and the literature on full cost pricing (see, for instance, Banker and Hughes (1994); Balakrishnan and Sivaramakrishnan (2002); Göx (2002)).

accounting for local and temporal variations in computing demand and the availability of wind and solar power.

Our paper contributes to the growing literature on decarbonization in several ways. First, recent empirical studies on corporate decarbonization have examined the drivers of firms' abatement efforts, including management targets (Ioannou et al., 2016), executive compensation (Cohen et al., 2023), governance changes (Dyck et al., 2023), shareholder engagement (Desai et al., 2023; Azar et al., 2021; Dyck et al., 2019), mandatory disclosure regulation (Downar et al., 2021; Tomar, 2023), and carbon pricing mechanisms (Jacob and Zerwer, 2024; Bai and Ru, 2024; Colmer et al., 2025). Recent work has also examined how companies reduce emissions, including investments in energy efficiency (Achilles et al., 2025) and divestiture from polluting assets (Berg et al., 2026). Our paper adds to this line of work by developing a model for managers to identify and implement specific technological and operational changes to substantially reduce actual emissions at least cost.

Second, Wang et al. (2013) have analyzed the optimal adoption of electric vehicles as fleet operators make capacity adjustments over time, while Naumov et al. (2023) and Shi et al. (2022) have examined the effectiveness of alternative policy instruments in accelerating this adoption.[4] More broadly, Drake et al. (2016) and Drake (2018) have studied how carbon pricing mechanisms shape a firm's decision to optimally invest in a low-carbon production technology. Islegen and Reichelstein (2011) have estimated the costs of adopting carbon capture technologies at fossil fuel power plants. Our study complements this work with an abatement cost model for assessing the costs of adopting and deploying low-carbon technologies required to meet specific emission targets or comply with environmental regulations. Central to our analysis is the development of three cost measures—total cost of ownership, total abatement cost, and levelized cost per mile—that allow management to steer an organization's decarbonization efforts.

Third, Glenk et al. (2026) develop an abatement cost model for the cost-efficient combination of discrete abatement levers at a single plant, where the costs and abatement effects of these levers are not additively separable. In contrast, our model characterizes the cost-

[4]Our paper also relates to the sizable literature in transportation research on the optimal configuration and operation of (electric) vehicle fleets (see, for instance, Perumal et al. (2022) for a recent review). It further relates to the numerous studies in the energy literature on the total cost of ownership of alternative drivetrain technologies in various applications (see, for instance, Noll et al. (2022); Avenali et al. (2023); Moon et al. (2025); Stolz et al. (2022); Woody et al. (2023)). To this line of work, our study contributes a model framework for assessing the cost of decarbonizing vehicle fleets and the effectiveness of alternative policy instruments in driving this transition.

efficient scale of a single abatement lever for each operating asset in the portfolio a firm seeks to decarbonize. We demonstrate that the costs and abatement effects of continuously expanding this lever, the electric drivetrain capacity, are additively separable across vehicles. This separability enables several analytical results unattainable in Glenk et al. (2026). In particular, we can characterize each asset's cost-efficient configuration in closed form, derive the marginal abatement cost curve directly from the firm's constrained optimization rather than from an ex-post ordering of levers, and show that the firm can decentralize this configuration through a single internal carbon price across asset managers. Overall, the two models address complementary abatement problems, and firms seeking to decarbonize multiple operating assets, each with several abatement levers, could ultimately implement a nested version of them.

The remainder of this paper is organized as follows. Section 2 analyzes the total cost of fleet ownership both analytically and numerically. Section 3 constructs the abatement cost curves for vehicle fleets, while Section 4 examines the impact of carbon pricing. Section 5 discusses our numerical findings, and Section 6 concludes. The Appendix provides proofs to our formal results, details on our data collection, additional numerical analysis, model extensions, and a discussion of alternative model applications.

2 Total Cost of Ownership

2.1 Model Framework

Our model considers a fleet operator serving a given demand for transportation services. This demand is represented by a matrix of n routes to be served across $m = 365$ days per year, where a route refers to the entire daily deployment of a vehicle. Each element $r_{ij} \geq 0$ of the matrix captures the total energy in kilowatt-hours (kWh) a vehicle requires to serve route $i = 1, \ldots, n$ on day $j = 1, \ldots, m$. Energy demand varies across routes and days due to factors such as speed, load, distance, traffic, temperature, and topography.[5] Our analysis assumes that the distribution of daily energy demand remains unchanged across years in the T-year planning horizon. Annual shifts in demand could be captured, for example, by specifying demand across $m = 365 \cdot T$ days.

[5]Our model is readily adapted to account for uncertainty in demand. The cost-efficient electric capacity of a vehicle is then determined based on the *expected* number of days with sufficiently large energy demand.

To serve each daily route r_{ij} with one vehicle, the firm initially seeks to acquire a fleet of n vehicles. We extend our model to settings where the firm already operates a legacy fleet in Appendix A4. Each vehicle $k = 1, \ldots, n$ may be equipped with up to two drivetrain technologies. While the model framework is generic, the following discussion will focus on battery-electric and diesel drivetrains. Combinations of the two drivetrains reflect plug-in hybrid vehicles, which are becoming available for heavy-duty applications. To capture differences in energy efficiency, we express r_{ij} in electric kWh, that is, the total energy a vehicle needs to charge to serve the route using the electric drivetrain. Parameters pertaining to diesel drivetrains will account for the additional energy required to serve the same route. Either drivetrain can be fully replenished at the end of each day.[6]

Vehicle drivetrains typically consist of an energy component (e.g., battery or fuel tank) and a power component (e.g., electric motors or combustion engine). Configurations range from pure electric systems with large batteries and motors to pure diesel systems with large tanks and engines. Hybrids span designs that are primarily diesel-powered with limited electric assistance to those that are primarily electric with a diesel generator for range extension. For notational parsimony, we initially represent the capacity size of a drivetrain with a single variable, approximating that vehicles with a larger energy component of a given drivetrain rely more on that drivetrain and are equipped with commensurate power capacity. We extend our model in Appendix A4 to include fixed costs for the power component of the drivetrains when installed. We thus denote the effective electric and diesel capacity of vehicle k in kWh by c_k^e and c_k^d, respectively, and the corresponding vector for all vehicles by $\vec{c}$. While diesel drivetrains are assumed to be capable of serving any demand, we introduce the constraint $c_k^e \leq \bar{c}_k^e$ to capture potential weight or space constraints for electric drivetrains. Our model initially ignores any temporal degradation of the operated assets, though it can be readily extended to capture potential degradation of battery capacity, as shown in Appendix A4.

Investment in the fleet entails capacity-related costs for the drivetrains and vehicles. We denote by v_k^e and v_k^d the acquisition cost (less the discounted salvage value) per kWh of effective electric and diesel capacity of vehicle k, respectively. Since electric drivetrains are typically more expensive to acquire, we specify that $v_k^e > v_k^d$. Consistent with our convention

[6]Our model can be extended to impose a penalty per kWh of unmet energy demand. The cost-efficient electric capacity of a vehicle is then determined as in Proposition 1. The cost-efficient diesel capacity is determined subsequently in a similar manner, based on the savings in variable costs from using the diesel drivetrains instead of paying the penalty. If the cost-efficient capacity of both drivetrains is equal to zero, the firm will prefer not to acquire the vehicle and incur the penalty instead.

that r_{ij} is expressed in electric kWh, v_k^d reflects the capacity-related costs per kWh of diesel capacity, adjusted for the additional energy required by a diesel drivetrain relative to an electric drivetrain to serve the same route. The drivetrain-independent capacity-related costs of vehicle k are denoted by v_k and include the acquisition cost, the discounted salvage value, and the discounted fixed operating costs, such as insurance, registration, and certain maintenance activities.

Variable operating costs also include components for the drivetrains and vehicles. We denote by w^e and w^d the cost of fuel and maintenance per kWh of energy provided by the electric and diesel drivetrains, respectively. Since electric drivetrains are typically cheaper to operate, we presume that $w^e < w^d$. Similar to v_k^d, w^d accounts for the energy inefficiency of diesel drivetrains relative to electric drivetrains. Both w^e and w^d are invariant across time and vehicles because fleet operators often have fixed-price purchase agreements with fuel suppliers.[7] The drivetrain-independent variable operating costs of a vehicle are given by w and include the prorated salary of drivers and maintenance activities.[8]

The total variable operating costs incurred will depend on the assignment of vehicles to routes and the deployment of drivetrains in each vehicle on those routes. The variable $x_{ijk} \in \{0, 1\}$ indicates whether vehicle k is assigned to daily route r_{ij}. The feasible set of assignments X consists of all assignments collected by the vector $\vec{x}$ such that each daily route is served by one vehicle (i.e., $\sum_{k=1}^{n} x_{ijk} = 1 \ \forall i, j$) and each vehicle is assigned to one daily route (i.e., $\sum_{i=1}^{n} x_{ijk} = 1 \ \forall j, k$). Similarly, let $q_{ijk}^e \in [0, c_k^e]$ and $q_{ijk}^d \in [0, c_k^d]$ denote the kWh of energy driven by vehicle k on route r_{ij} with the electric and diesel drivetrains, respectively, and let the vector $\vec{q}$ collect all deployments. The feasible set of deployments Q requires each daily route to be fully served (i.e., $q_{ijk}^e + q_{ijk}^d \geq r_{ij} \cdot x_{ijk} \ \forall i, j, k$).

The firm seeks to minimize the total cost of acquiring a fleet of vehicles with electric and diesel drivetrains, assigning vehicles to routes across days in the planning horizon, and deploying the drivetrains on each daily route. Incentives for investing in electric drivetrains

[7] If w_j^e and w_j^d vary across days j but satisfy $w_j^e < w_j^d$ for all j, Lemma 1 below continues to apply. In contrast, if w_k^e and w_k^d vary across vehicles k, the cost matrix in the underlying assignment problem no longer satisfies the Monge property used in the proof of Lemma 1. Standard numerical algorithms for linear sum assignment problems can then identify the cost-efficient deployment.

[8] If firms are uncertain about costs, each cost parameter v_k^e, v_k^d, v, w^e, w^d, and w can be reinterpreted as the expected value of the underlying random variables. For a risk-neutral decision-maker, the resulting $TCO(\cdot)$ function in equation (1) then represents the expected total cost of ownership. This cost will be minimized by the same capacity and deployment choices that minimize the deterministic $TCO(\cdot)$ when the cost parameters assume their expected values for sure, irrespective of the underlying probability distributions.

arise from avoiding expenditures for using diesel drivetrains. Yet, these savings in variable costs attainable over the life cycle of each vehicle must be traded off against higher upfront capital expenditures for electric drivetrains. Let $A(\delta, T) \equiv \sum_{t=1}^{T}(1+\delta)^{-t}$ denote the annuity value of \$1.0 paid over T years at the applicable cost of capital δ, where δ can be interpreted as the weighted average cost of capital. Given feasible drivetrain capacity sizes (i.e., Q is non-empty), the *Total Cost of Ownership* (TCO) for the vehicle fleet is given by:

$$\begin{aligned} TCO(\vec{c}) \equiv & \sum_{k=1}^{n}\Big[v_k + v_k^e \cdot c_k^e + v_k^d \cdot c_k^d\Big] + A(\delta, T) \cdot \\ & \min_{\substack{\vec{x}\in X \\ \vec{q}\in Q}}\left\{\sum_{k=1}^{n}\sum_{i=1}^{n}\sum_{j=1}^{m} x_{ijk} \cdot \Big[(q_{ijk}^e + q_{ijk}^d)\cdot w + q_{ijk}^e \cdot w^e + q_{ijk}^d \cdot w^d\Big]\right\}. \end{aligned} \tag{1}$$

Since $w^e < w^d$, it will be more cost-effective for the firm to assign vehicles with larger electric capacity to daily routes with higher energy demand and to use the electric drivetrain first on each daily route. Accordingly, we can sort all vehicles by weakly decreasing electric capacity and relabel the index k so that $c_1^e \geq \ldots \geq c_n^e$. At the same time, suppose vehicle-to-route assignments are separable across days, as is typically the case for fleets returning to central depots overnight. We can then sort all routes on each day j by weakly decreasing energy demand and relabel the index i so that $r_{1j} \geq \ldots \geq r_{nj}$.[9]

Lemma 1. *The cost-efficient assignment of vehicle k on day j is $x_{ijk}^* = 1$ if and only if $i = k$ and zero otherwise. The corresponding cost-efficient drivetrain deployments are $q_{ijk}^{e*} = \min\{r_{ij}, c_k^e\}$ and $q_{ijk}^{d*} = \big(r_{ij} - \min\{r_{ij}, c_k^e\}\big)$.*

Lemma 1 follows from expressing equation (1) as a standard linear sum assignment problem (Burkard et al., 2009).[10] It implies that we can drop index k and use index i for both routes and vehicles. In addition, the search for the cost-efficient drivetrain capacity can be performed separately for each vehicle. This is because each vehicle is dedicated to a particular route and hence independent of other vehicles. The search can also focus on the cost-efficient electric capacity of a vehicle, while the size of the corresponding diesel drivetrain will be equal to the largest of any remaining route segments. The firm's objective is

[9] If routes are interdependent across days, as is the case for fleets operating distinct multi-day trips, routes can be sorted and indexed so that $\sum_{j=1}^{m} r_{1j} \geq \ldots \geq \sum_{j=1}^{m} r_{nj}$.

[10] The proofs for all formal results are relegated to Appendix A1.

then to minimize the total cost of ownership for each vehicle i given by:

$$TCO_i(c_i^e) \equiv a_i + c_i^e \cdot (v_i^e - v_i^d) - A(\delta, T) \cdot (w^d - w^e) \cdot \sum_{j=1}^{m} \min\{r_{ij}, c_i^e\}, \tag{2}$$

where

$$a_i \equiv v_i + \max_j \{r_{ij}\} \cdot v_i^d + A(\delta, T) \cdot (w + w^d) \cdot \sum_{j=1}^{m} r_{ij}.$$

By construction, $TCO(\vec{c}) = \sum_{i=1}^{n} TCO_i(c_i^e)$.

Lemma 2. *$TCO_i(\cdot)$ is a piecewise linear and convex function of c_i^e.*

The claim in Lemma 2 follows directly from the observation that for any r_{ij} the term $\min\{r_{ij}, c_i^e\}$ is piecewise linear and concave in c_i^e, and therefore $-A(\delta, T) \cdot (w^d - w^e) \cdot \sum_{j=1}^{m} \min\{r_{ij}, c_i^e\}$ is a convex function of c_i^e. Lemma 2 reflects that as the electric capacity c_i^e increases, the capacity-related costs of vehicle i rise linearly. The associated savings in variable costs attainable over the life cycle also grow linearly, as long as the set of days with energy demand $r_{ij} \geq c_i^e$ remains unchanged. Once c_i^e exceeds a particular r_{ij}, this set contracts, and the additional electric capacity yields the per-unit savings on fewer days. As a result, the total cost of ownership for the vehicle increases more steeply. Each of these breakpoints of the $TCO_i(\cdot)$ function corresponds to a distinct value of the daily energy demand levels served by the vehicle.

To identify the electric capacity minimizing the $TCO_i(\cdot)$ function, the *Marginal Cost of Ownership* (MCO) for vehicle i at any $c_i^e > 0$ is then given by the left-derivative of the $TCO_i(\cdot)$ function (at $c_i^e = 0$, it is given by the right-derivative). Thus:

$$MCO_i(c_i^e) = (v_i^e - v_i^d) - A(\delta, T) \cdot (w^d - w^e) \cdot I_i(c_i^e), \tag{3}$$

where $I_i(c_i^e) \equiv \sum_{j=1}^{m} \mathbb{1}\{r_{ij} \geq c_i^e\}$, with the indicator function $\mathbb{1}\{a \geq b\} = 1$ if $a \geq b$ and zero otherwise. $I_i(c_i^e)$ counts the days per year with energy demand $r_{ij} \geq c_i^e$, that is, the days on which vehicle i yields the full variable cost savings from using the electric drivetrain. $I_i(\cdot)$ is a weakly decreasing, left-continuous step function in c_i^e, such that $I_i(0) = 365$. Assuming that $(r_{i1}, \ldots, r_{im})$ entails $m_i^+ \leq m$ distinct positive values and denoting by r_i^u the u-th largest entry in the vector $(r_{i1}, \ldots, r_{im})$, we have $I_i(r_i^u) = u$ for $1 \leq u \leq m_i^+$.

The cost-efficient electric capacity of vehicle i is then equal to zero if $MCO_i(0) > 0$, while it is equal to $\min\{r_i^1, \bar{c}_i^e\}$ if $MCO_i(r_i^1) = (v_i^e - v_i^d) - A(\delta, T) \cdot (w^d - w^e) \leq 0$. If neither

of these cases applies, the cost-efficient electric capacity is an interior solution given by the value at which $MCO_i(\cdot)$ changes sign. To identify this value, we solve equation (3) for $I_i(\cdot)$ at $MCO_i(\cdot) = 0$ and obtain:

$$\lambda_i \equiv \frac{v_i^e - v_i^d}{A(\delta, T) \cdot (w^d - w^e)}. \tag{4}$$

We refer to the scalar λ_i as the *critical utilization* of the electric capacity of vehicle i. It is given by the vehicle's cost profile and captures the number of days per year that the marginal unit of electric capacity must be used so that the life-cycle variable cost savings are exactly equal to the additional capacity-related costs. Intuitively, λ_i declines with falling capacity-related costs of electric drivetrains v_i^e, increasing variable costs of diesel drivetrains w^d, and a declining cost of capital δ.

Proposition 1. *For each vehicle i, the cost-efficient electric capacity is given by:*

(i) $c_i^{e*} = 0$ *if* $\lambda_i > m_i^+$,

(ii) $c_i^{e*} = \min\{r_i^u, \bar{c}_i^e\}$ *if* $u - 1 < \lambda_i \leq u$, *with* $u \in \{1, \ldots, m_i^+\}$.

Proposition 1 shows that the cost-efficient configuration of each vehicle can be identified by comparing its critical utilization with its *load duration curve* given by the mapping $L_i(u) = r_i^u$. This curve reflects the ordered demand profile the vehicle must satisfy, meaning that the energy demand for vehicle i was at least r_i^u for u days, with $1 \leq u \leq m_i^+$. The load duration curve can be extended to the entire interval of real numbers $[0, m_i^+]$ by setting $L_i(t) = r_i^u$ if $u - 1 \leq t \leq u$.

Figure 1 illustrates Proposition 1 by plotting the load duration curve of vehicle i, i.e., its daily energy demands r_{ij} sorted in descending order, against the days of the year. The intersection of this curve with the critical utilization of the electric capacity then identifies the cost-efficient electric capacity of vehicle i, that is, $c_i^{e*} = L_i(\lambda_i) = r_i^u$, provided $u - 1 \leq \lambda_i \leq u$. This approach mirrors the use of electricity load duration curves in the energy sector to identify the cost-efficient combination of power generation technologies required to meet a given, time-variant electricity demand (Hu et al., 2015; Kök et al., 2020).

Figure 1 also highlights that the cost-efficient configuration of each vehicle is governed by the shape of its load duration curve. Concave (parts of) load duration curves reflect baseload operations and favor electric capacity, while convex (parts of) load duration curves reflect peaker operations and favor diesel capacity. Load duration curves become even more

significant when both v_i^e and v_i^d are invariant across vehicles, for example, because all vehicles in the fleet belong to the same class. In that case, the fleet operator computes the critical utilization once, $\lambda_i = \lambda$, and plugs it into each vehicle's load duration curve.

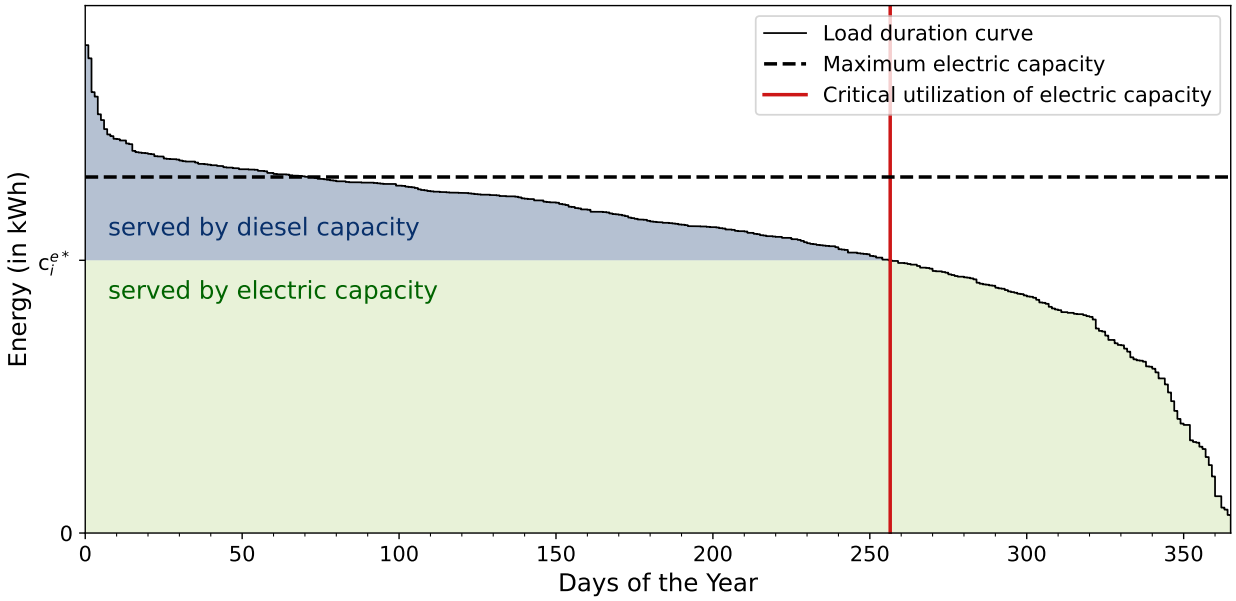


Figure 1. Cost-efficient configuration and deployment of a vehicle. This figure illustrates the load duration curve, critical utilization of the electric capacity, cost-efficient electric and diesel capacity, and cost-efficient deployment of the drivetrains of vehicle i.

2.2 Application to Urban Bus Fleets

We calibrate our model framework throughout the paper to urban bus fleets in the current economic context of California. Urban buses are heavy-duty vehicles that contribute not only to global carbon emissions but also to local air pollution in populated areas. They typically operate on regular duty cycles, serving similar routes across the days and weeks of a year. As part of these duty cycles, they usually return to central depots overnight for cleaning, refueling/recharging, and other daily maintenance activities. Public transit agencies have also been among the first fleet operators to replace diesel-powered vehicles with alternatives such as plug-in hybrids and battery-electric buses (BNEF, 2025).

Our data on daily routes to be served stems from detailed operational records of a public transit agency in California. This agency serves an extensive metropolitan area with diverse routes, using a fleet of over 600 buses. The operational data available to us includes daily records of nearly 100 buses in the fleet for the entire year of 2022. Based on this data, we

obtain the daily energy demand of routes to be served by the vehicle fleet in our analysis. This energy demand reflects the actual daily mileage of buses in the dataset, including any deviations from the scheduled duty cycle. Details about the data and the collection process are provided in Appendix A2. For clarity, our analysis focuses on a subset of 50 vehicles that captures the distribution of regular operational profiles in the data.

Table 1. Main cost and operational parameters.

in 2024 $US	**Electric**	**Diesel**
Capacity-related costs of drivetrains ($/kWh)	360	8.45
Variable costs of drivetrains ($/kWh)	0.13	0.30
Maximum drivetrain capacity (kWh)	549	–
Capacity-related costs of vehicles ($)	635,495	
Variable costs of vehicles ($/kWh)	0.23	
Useful lifetime (years)	12	
Cost of capital (%)	7	

We complement the route data with cost and operational information obtained from expert interviews, technical reports, and peer-reviewed academic articles. Table 1 shows the main cost and operational parameters for the electric and diesel drivetrains and the vehicles themselves (see Supplementary Data for details). Since the urban bus service provider serves all routes in our dataset with the same bus type (40-ft standard bus), we use the same capacity-related costs for all vehicles. The capacity-related costs of the electric drivetrain account for a maximum depth of discharge of 80%, which increases the unit cost of the usable battery pack. As described above, the capacity-related costs and the variable cost of the diesel drivetrain are adjusted for the energy inefficiency of diesel drivetrains relative to electric drivetrains. The variable costs of the vehicles exclude driver salaries, which are the same across drivetrains. Following the lead of public transportation experts, we set the weighted average cost of capital at 7.0% and the useful life of vehicles at 12 years.

Figure 2a shows the load duration curves of all buses in the fleet as black lines. They result from the cost-efficient deployment of drivetrains on routes described in Lemma 1, presuming that repairs and maintenance can occur overnight at the central depot.[11] While the load duration curves exhibit substantial heterogeneity in magnitude and shape across buses, most are concave on the right-hand side and convex on the left-hand side. The red vertical line indicates the critical utilization of the electric capacity of the buses. As per Proposition 1,

[11] Appendix A3 identifies the cost-efficient bus fleet when each bus is restricted to its observed deployment.

the cost-efficient electric capacity of each bus is then determined by the lower of either the energy demand at the intersection of its load curve (black line) with the critical utilization of the electric capacity (red line) or the maximal electric capacity (horizontal dashed line). If no intersection occurs, the cost-efficient electric capacity is zero.

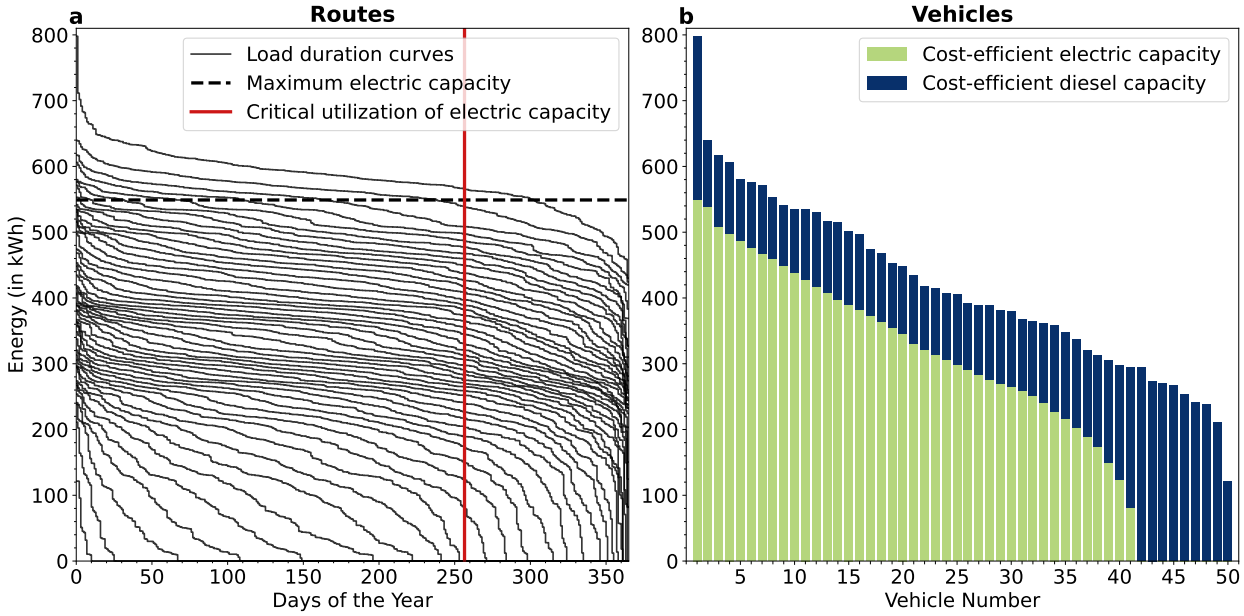


Figure 2. Cost-efficient urban bus fleet. This figure shows (**a**) the load duration curves of buses in the fleet and (**b**) the cost-efficient capacity of the electric and diesel drivetrains of the buses.

Figure 2b shows the corresponding capacity sizes of the drivetrains. We find that the cost-efficient fleet consists of 41 plug-in hybrid, nine diesel, and no fully electric buses. This reflects that nine buses operate too infrequently to reach the critical utilization threshold of 256 days, while 41 buses exhibit high energy demand on fewer than 256 days per year. For the hybrid buses, the cost-efficient electric capacity ranges between 81–549 kWh (28–84% of the total energy capacity of the vehicles), with an average of 337 kWh (72%). Consistent with the shape of their load duration curves, most are primarily electric with a diesel generator for range extension, while the buses starting near vehicle number 40 are primarily diesel buses. Overall, the cost-efficient fleet has a total electric capacity of 13,801 kWh (66% of the total energy capacity) and serves 4,813 Megawatt-hours (MWh, 88% of the total energy demand) annually using that capacity. These totals highlight that electric drivetrains operate as baseload capacity, while diesel drivetrains serve as peaker capacity.

3 Abatement Cost Curves

3.1 Model Framework

Operating a vehicle fleet causes emissions that impose external costs on the environment. We now embed the preceding model in a decision context where fleet operators seek to reduce their annual emissions to meet a given emission target. This target may stem from a voluntary climate pledge or a regulatory mandate such as a registration ban or performance standard. Consistent with such environmental regulations, our analysis will focus on direct (Scope 1) emissions from powering vehicles with fossil fuels, measured in tons of carbon dioxide equivalents (CO_2e).[12]

Our analysis presumes that the cost-efficient vehicle fleet identified via Proposition 1 includes conventional drivetrains, as is the case for almost all vehicle fleets today. We denote by θ the tons of CO_2e emitted per kWh of energy driven by diesel drivetrains. Similar to v_i^d and w^d, θ is adjusted for the energy inefficiency of diesel drivetrains relative to electric drivetrains. Since electric drivetrains emit no direct emissions, the annual direct emissions from operating the cost-efficient vehicle fleet are given by $E_0 \equiv \sum_{i=1}^{n} E_i(c_i^{e*})$, where

$$E_i(c_i^e) \equiv \sum_{j=1}^{m} \big(r_{ij} - \min\{r_{ij}, c_i^e\}\big) \cdot \theta. \tag{5}$$

A feasible target E lies in the interval $[E_-, E_0]$, where $E_- \equiv \sum_{i=1}^{n} E_i(\bar{c}_i^e)$ reflects the minimal annual emissions attainable when each vehicle is equipped with the largest possible electric capacity. Let $C(E) \equiv \{\vec{c} \mid \sum_{i=1}^{n} E_i(c_i^e) \leq E\}$ be the set of all feasible vectors $\vec{c}$ resulting in the fleet's future annual emissions not exceeding E. For any given target E, the firm then seeks to identify the vector $\vec{c} \in C(E)$ that minimizes the fleet's total cost of ownership associated with achieving that emissions level.

The *Total Abatement Cost* (TAC) of reducing annual emissions from E_0 to E is then

[12] Greenhouse gases other than CO_2 can be converted to CO_2e using generally accepted conversion factors. Our analysis extends to indirect (Scope 2) emissions embodied in electricity used to power electric drivetrains by augmenting $E_i(c_i^e)$ in equation (5) with a term proportional to the emission rate of purchased electricity. When this rate is positive but below the diesel emission rate, our analysis proceeds as in the current one, with higher fleet emissions. When the rate is equal to zero, for example, because the firm verifies that all electricity consumed is renewable, our analytical and numerical findings remain unchanged.

defined as:

$$\begin{aligned} TAC(E|E_0) &\equiv \min_{\vec{c}\in C(E)} \sum_{i=1}^{n} TCO_i(c_i^e) \; - \min_{\vec{c}\in C(E_0)} \sum_{i=1}^{n} TCO_i(c_i^e), \\ &= \min_{\vec{c}\in C(E)} \sum_{i=1}^{n} TCO_i(c_i^e) \; - \sum_{i=1}^{n} TCO_i(c_i^{e*}). \end{aligned} \tag{6}$$

Given annual emissions of E_0, $TAC(E|E_0)$ reflects the minimal payment that a firm would require for its investments and operating costs to serve the same routes with no more than E metric tons of CO_2e per year for the next T years. By construction, $TAC(E_0|E_0) = 0$.

Proposition 2. *$TAC(\cdot\,|E_0)$ is a decreasing piecewise linear and convex function of E.*

Proposition 2 reflects that the firm expands electric capacity first where it lowers emissions at least cost, so each additional ton of CO_2e abated costs weakly more than the last. Formally, the $TAC(\cdot\,|E_0)$ curve represents the value of the minimized sum $\sum_{i=1}^{n} TCO_i(c_i^e)$ subject to the constraint that $\sum_{i=1}^{n} E_i(c_i^e) \leq E$. Since each $TCO_i(\cdot)$ function is piecewise linear and convex in c_i^e (see Lemma 2), and each of the component constraint functions $E_i(\cdot)$ is piecewise linear and convex in c_i^e (see equation (5)), it is straightforward to verify that the minimized value function $TAC(\cdot\,|E_0)$ is piecewise linear and convex in the aggregate constraint E.

Each breakpoint of the $TAC(\cdot\,|E_0)$ curve marks the end of a linear segment. Tightening the emission target along such a segment increases the cost-efficient electric capacity of a subset of vehicles up to their respective next largest demand thresholds r_i^u (or $\bar{c}_i^e$). At these thresholds, the $TCO_i(\cdot)$ and $E_i(\cdot)$ functions of the vehicles exhibit a breakpoint. Once all vehicles in the subset reach their respective thresholds, the $TAC(\cdot\,|E_0)$ curve exhibits a breakpoint. We denote the breakpoints by $E_- = E_s < \ldots < E_0$. Our subsequent analysis restricts the choice of the target E to one of these breakpoints, as they are typically densely spaced in practice (see Figure 3).

On the domain of these breakpoints, we define the *Marginal Abatement Cost* (MAC) curve corresponding to the $TAC(\cdot\,|E_0)$ curve as the difference quotient associated with reducing annual emissions from E_{k-1} to E_k over the planning horizon. Formally, for $1 \leq k \leq s$:

$$MAC(E_k) \equiv \frac{TAC(E_k|E_0) - TAC(E_{k-1}|E_0)}{(E_{k-1} - E_k) \cdot A(\delta, T)} \equiv \frac{TAC(E_k|E_{k-1})}{(E_{k-1} - E_k) \cdot A(\delta, T)}. \tag{7}$$

Including the annuity factor $A(\delta, T)$ in the denominator ensures that the life-cycle cost of reducing annual emissions is divided by the corresponding life-cycle reduction in emissions.

The $MAC(\cdot)$ curve defined in equation (7) is structurally related to classical marginal abatement cost curves popularized by the consulting firm McKinsey (2007) and studied in environmental economics (Stavins, 2019; Grubb et al., 2014; Beaumont and Tinch, 2004). These curves are constructed by calculating the unit cost and abatement effect of discrete levers a firm can implement to reduce emissions and reordering them by their unit cost. In contrast, our $MAC(\cdot)$ curve is derived from the $TAC(\,\cdot\,|E_0)$ curve as the difference quotient associated with reducing annual emissions from one breakpoint to the next. Each breakpoint can be uniquely identified with a subset of vehicles that exhibit the same marginal abatement cost of increasing their electric capacity to their respective next largest energy demand threshold r_i^u (or $\bar{c}_i^e$). If these subsets are interpreted as discrete levers, our $MAC(\cdot)$ curve corresponds to a classical marginal abatement cost curve.

To identify the electric capacity across vehicles constituting the $TAC(\,\cdot\,|E_0)$ curve, that is, minimizing $\sum_{i=1}^n TCO_i(c_i^e)$ subject to the fleet-wide emission constraint $\sum_{i=1}^n E_i(c_i^e) \leq E_k$, we form the corresponding Lagrangian:

$$\mathcal{L}(\mu, \vec{c}) \;=\; \sum_{i=1}^{n} TCO_i(c_i^e) \;+\; \mu\Big(\sum_{i=1}^{n} E_i(c_i^e) - E_k\Big), \tag{8}$$

where $\mu \geq 0$ denotes a Lagrange multiplier for the emission constraint. With differentiable objective and constraint functions, the Kuhn-Tucker theorem implies that there exists a non-negative multiplier such that an optimal solution to the constrained problem can be obtained by minimizing the unconstrained Lagrangian. The following analytical result extends this approach to a piecewise differentiable convex objective and constraint functions. Since the resulting multiplier is not unique, we denote by $\mu(E_k)$ the slope of the linear segment of the $TAC(\,\cdot\,|E_0)$ function ending at E_k.

Lemma 3. *For any emission target E_k, an optimal solution to the objective of minimizing $\sum_{i=1}^n TCO_i(c_i^e)$ subject to the constraint $\sum_{i=1}^n E_i(c_i^e) \leq E_k$ is obtained by minimizing the Lagrangian $\mathcal{L}(\mu(E_k), \vec{c})$ over $\vec{c}$. Further, $\mu(E_k)$ satisfies:*

$$\mu(E_k) = MAC(E_k) \cdot A(\delta, T),$$

for $k = 1, \ldots, s$, while $\mu(E_0) = 0$.

Lemma 3 follows from two observations. First, the constrained cost minimization can be formulated as a feasible and bounded linear program, so a Kuhn-Tucker multiplier exists and

the Kuhn-Tucker theorem applies (Rockafellar, 1997). Second, this multiplier captures the marginal increase in minimized cost $\sum_{i=1}^{n} TCO_i(c_i^e)$ resulting from tightening the emission constraint $\sum_{i=1}^{n} E_i(c_i^e) \leq E_k$. Since this minimized cost, or equivalently the $TAC(\cdot|E_0)$ curve, is piecewise linear in E (see Proposition 2), the multiplier would be unique and equal to the negative slope of the $TAC(\cdot|E_0)$ curve whenever the emission target were to lie strictly between two breakpoints. At a breakpoint, the $TAC(\cdot|E_0)$ curve is not differentiable, and an admissible multiplier can take any value between the two adjacent negative slopes, including the boundary value $\mu(E_k)$ (Rockafellar, 1997).

The cost-efficient electric capacity of each vehicle i given the fleet-wide emission target E_k can then be identified in direct analogy to the unconstrained optimization in Section 2.1. Since the Lagrangian in equation (8) is separable across vehicles (see Lemma 1), the firm's objective is to choose c_i^e for vehicle i so as to minimize:

$$TCO_i(c_i^e) + \mu(E_k) \cdot E_i(c_i^e). \tag{9}$$

The corresponding left-derivative at any $c_i^e > 0$ (right-derivative at $c_i^e = 0$) is given by:

$$MCO_i(c_i^e) - \mu(E_k) \cdot \theta \cdot I_i(c_i^e). \tag{10}$$

The cost-efficient electric capacity of vehicle i is equal to c_i^{e*} if $MCO_i(c_i^{e*}) - \mu(E_k) \cdot \theta \cdot I_i(c_i^{e*}) > 0$. Alternatively, it is equal to $\min\{r_i^1, \bar{c}_i^e\}$ if $MCO_i(r_i^1) - \mu(E_k) \cdot \theta \cdot I_i(r_i^1) \leq 0$. If neither of these cases applies, the cost-efficient electric capacity is an interior solution given by a value at which the expression in equation (10) changes sign. When multiple such values exist, we presume that the firm selects the largest electric capacity. To identify this capacity, we set equation (10) equal to zero, solve for $I_i(c_i^e)$, and obtain:

$$\lambda_i(E_k) \equiv \frac{v_i^e - v_i^d}{A(\delta, T) \cdot (w^d - w^e) + \mu(E_k) \cdot \theta}. \tag{11}$$

We refer to the scalar $\lambda_i(E_k)$ as the critical utilization of the electric capacity of vehicle i, given the fleet-wide emission target E_k. We note that $\lambda_i(E_k) \leq \lambda_i$, as the term $\mu(E_k) \cdot \theta$ increases the effective benefit of electrification by valuing avoided emissions at the shadow price $\mu(E_k)$. As the emission target E_k tightens, $\mu(E_k)$ increases and $\lambda_i(E_k)$ declines, making additional electric capacity cost-efficient at lower utilization levels. If the emission constraint is slack, $\mu(E_k) = 0$ and $\lambda_i(E_k) = \lambda_i$.

Proposition 3. *For any emission target E_k, the cost-efficient electric capacity of each vehicle i that results in annual direct emissions of the fleet not exceeding E_k is given by:*

(i) $c_i^{e*}(E_k) = 0$ *if* $\lambda_i(E_k) > m_i^+$,

(ii) $c_i^{e*}(E_k) = \min\{r_i^u, \bar{c}_i^e\}$ *if* $u - 1 < \lambda_i(E_k) \leq u$, *with* $u \in \{1, \ldots, m_i^+\}$.

Proposition 3 determines the cost-efficient fleet through the same rule as Proposition 1, under which the firm compares each vehicle's load duration curve against a single critical utilization threshold. The main difference is that an emission target lowers this threshold from λ_i to $\lambda_i(E_k)$ by valuing avoided emissions at the shadow price $\mu(E_k)$. Without a target, λ_i depends only on vehicle i's cost profile, so each vehicle is configured independently of the others. With a target, $\lambda_i(E_k)$ depends on the fleet-wide shadow price $\mu(E_k)$, so any one vehicle's configuration now also depends on the relative distribution of load duration curves across the fleet.

For a given emission reduction target E_k, concave (convex) load duration curves require smaller (larger) increases in cost-efficient electric capacity $c_i^{e*}(E_k)$ of the corresponding vehicles, where the additional electric capacity is used more (less) frequently. This implies smaller (larger) increases in marginal abatement cost $MAC(E_k)$ and the shadow price $\mu(E_k)$, and thus smaller (larger) decreases in critical utilization rates $\lambda_i(E_k)$. To see this graphically, note that the emissions of a vehicle are given by the area under its load duration curve served by diesel capacity multiplied with the carbon intensity factor θ (see Figure 1).

3.2 Application to Urban Bus Fleets

The carbon intensity of diesel drivetrains is estimated at $\theta = 0.82$ kilogram (kg) of CO_2e per kWh (see Appendix A2 for details). Figure 3a shows the total abatement cost of reducing the annual emissions of the urban bus fleet from E_0 to a target E_k. We depict the total abatement cost in annualized form, that is, $TAC(\cdot\,|E_0) \cdot A(\delta, T)^{-1}$, since our focus lies on annual emission reductions. The baseline $E_0 = 543$ tCO_2e corresponds to the cost-efficient fleet in Figure 2b. In contrast, the lowest feasible level at $E_- = 21.95$ tCO_2e (4% of E_0) reflects a fleet with near-complete electrification. That is, all vehicles are fully electric except vehicles 1–8 in Figure 2b, which are capped at the maximal feasible electric capacity of 549 kWh. Consistent with Proposition 2, the total abatement cost curve is piecewise linear and convex. It appears smooth only because the $s = 256$ breakpoints are densely spaced.

Figure 3a predicts that the total abatement costs rise steeply as firms pursue more ambitious emission targets. For example, reducing emissions by up to 10% from 543 tCO_2e to 489 tCO_2e incurs annualized abatement costs of less than \$239. In contrast, a reduction of more than 90% to less than 54 tCO_2e entails annualized abatement costs of more than \$66,827. Yet, even the most ambitious emission targets impose relatively modest costs when viewed against the total cost of fleet ownership. To calibrate, the annualized total abatement cost at E_- amounts to \$175,924, which is equivalent to 2.6% of the annualized total cost of ownership for the cost-efficient fleet in Figure 2b. In other words, relative to the cost-efficient fleet, firms could almost fully decarbonize their urban bus fleet for an increase in total cost of ownership of only 2.6%.

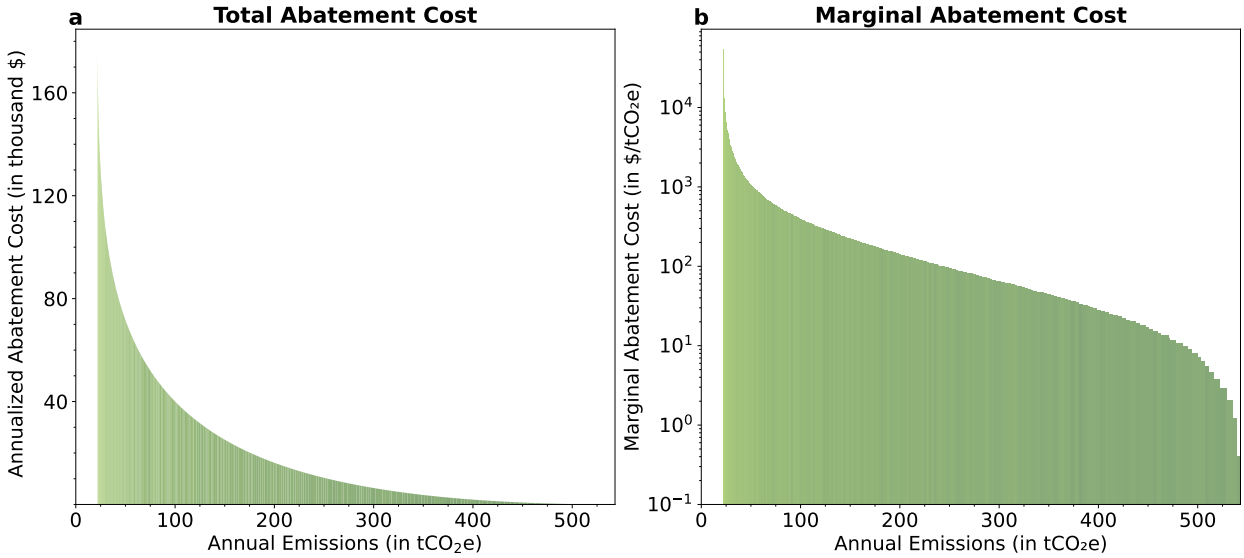


Figure 3. Abatement cost curves for urban buses. This figure shows (**a**) the annualized total abatement cost and (**b**) the marginal abatement cost for the urban bus fleet.

Figure 3b shows the corresponding marginal abatement cost curve. A striking property of this curve is its wide range of values that reflect a rotated S-shape when displayed on a logarithmic scale. In particular, reducing emissions by up to 10% from 543 tCO_2e to 489 tCO_2e incurs a relatively sharp increase in marginal abatement costs from \$0.4/tCO_2e to \$8.98/tCO_2e. Similarly, reducing emissions by more than 90% from 54 tCO_2e to 21.95 tCO_2e entails an even sharper relative increase from \$915/tCO_2e to \$53,800/tCO_2e. These increases reflect convex tails of the load duration curves of certain vehicles in the fleet. As the emission target is tightened along these tails, meeting the target requires substantial increases in the electric capacity of the vehicles, yet this additional capacity is utilized on only a few days of

high demand per year. Between the two extremes, the marginal abatement costs increase at a fairly constant rate of about 2.3% for every 1.0% reduction in emissions.

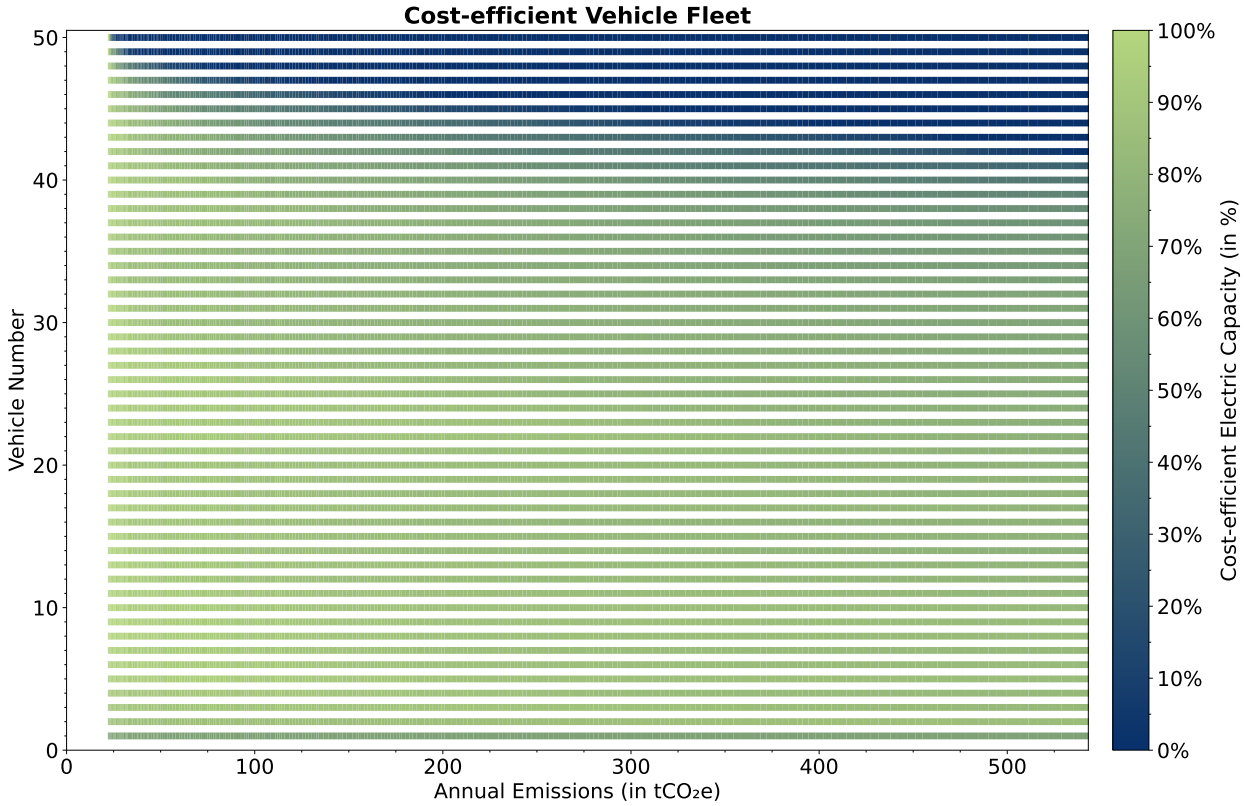


Figure 4. Cost-efficient decarbonization of urban buses. This figure shows the cost-efficient configuration of buses in the fleet corresponding to different emission levels.

Figure 4 shows the cost-efficient configuration of buses at different emission levels. Each horizontal bar represents one bus, with the color at particular emission levels indicating the share of the electric capacity of the total energy capacity of the bus. The configuration at $E_0 = 543$ tCO_2e corresponds to the cost-efficient fleet in Figure 2b. As firms seek to decarbonize, the cost-efficient strategy is to first expand the electric capacity of plug-in hybrid buses with relatively low initial electrification. Then, diesel buses are gradually electrified, starting with those used most frequently. These buses shift from primarily diesel drivetrains with limited electric support to primarily electric drivetrains with auxiliary diesel capacity for range extension. Maximal decarbonization requires expanding the electric capacity of all buses to their peak energy demand or maximum feasible level.

4 Impact of Carbon Pricing

4.1 Model Framework

Beyond emission targets, transport companies in California, the European Union, and other jurisdictions face charges on greenhouse gas emissions.[13] These charges may reflect a tax or market prices for emission permits under a cap-and-trade system, such as the California Cap-and-Trade Program and the European Emissions Trading System. Incentives for emissions reductions then result from the avoided expenditures for emission charges. Yet, firms must trade off these savings against the costs of emission abatement.

If a firm expects a charge of p per ton of CO_2e over the next T years, it seeks to choose emission level E to minimize:

$$TAC(E|E_0) - p \cdot (E_0 - E) \cdot A(\delta, T). \tag{12}$$

The following analytical result presumes that the firm selects the lowest emission level if multiple levels are optimal.[14]

Proposition 4. *For any emission charge p, the optimal annual direct emissions $E^*(p)$ of the vehicle fleet is:*

$$E^*(p) = E_k \text{ if and only if } MAC(E_{k+1}) > p \geq MAC(E_k) \text{ for some } k = 1, \ldots, s-1.$$

Alternatively, $E^*(p) = E_0$ if and only if $MAC(E_k) > p$, while $E^*(p) = E_s$ if and only if $p \geq MAC(E_s)$.

The inequalities in Proposition 4 reflect the discrete analog of the standard first-order condition equating marginal revenue and marginal cost. For the emissions level E_k to be optimal, the unit revenue from avoided emission charges, p, must be greater than or equal to the marginal cost of reducing emissions from E_{k-1} to E_k. Yet, this unit revenue must also be less than the marginal cost of reducing emissions from E_k to E_{k+1}. Proposition 4 also reflects the price-based analog of Lemma 3. While Lemma 3 characterizes a (life-cycle)

[13] In California, the transport sector was included in the Cap-and-Trade Program in the second compliance period (2015-2027) (Kynett, 2024). In the European Union, aviation and maritime shipping are already covered by the European Emissions Trading System, while road transport will fall under a separate system (called "ETS2") scheduled to become operational in 2027 (The European Commission, 2025).

[14] Alternatively, $E^*(p) = E$, for any $E \in [E_k, E_{k-1}]$ if and only if $p = MAC(E_k)$ for some $k = 1, \ldots, s$.

shadow price $\mu(E_k)$ corresponding to setting the emission constraint to E_k, Proposition 4 identifies the optimal emission level E_k induced by the external carbon price p. As such, $p \cdot A(\delta, T)$ can be viewed as an admissible Kuhn-Tucker multiplier at E_k. The cost-efficient electric capacity choices for each vehicle induced by the carbon price p can then be identified via Proposition 3 evaluated at the optimal emission level $E^*(p)$.

The elasticity of the firm's emission response to carbon prices, that is, the shape of the $E^*(\cdot)$ function, structurally depends on the load duration curves of vehicles in the fleet. For a given increase in emission charge p, and the associated reductions in critical utilization rates, concave (convex) load duration curves lead to larger (smaller) increases in cost-efficient electric capacity of the corresponding vehicles and to larger (smaller) reductions in emissions $E^*(p)$. Accordingly, concave (convex) load duration curves imply a higher (lower) elasticity of the firm's emission response to carbon prices. Importantly, a higher (lower) abatement elasticity means that a smaller (larger) increase in carbon prices is required to induce a desired emission reduction.

The characterization in Propositions 3 and 4 also shows how the firm can decentralize the fleet-wide capacity problem to its individual vehicle managers. Suppose the central unit assigns vehicles to routes according to Lemma 1 and sets an internal carbon price equal to p. Each vehicle manager then chooses c_i^e to minimize $TCO_i(c_i^e) + p \cdot A(\delta, T) \cdot E_i(c_i^e)$. The resulting capacity choices coincide with the centralized cost-efficient ones and therefore reproduce the optimal fleet emissions $E^*(p)$ in Proposition 4. For a fleet-wide emission target E_k, the same logic applies with the internal carbon price set equal to the shadow price $\mu(E_k)$ in Lemma 3, recovering the cost-efficient capacity choices in Proposition 3. This decentralization is robust to vehicle-specific cost information being private to the respective vehicle manager. The internal carbon price thus provides a coordination instrument for capacity management in the spirit of the managerial accounting literature on decentralized investment decisions (Baldenius et al., 2007; Dutta and Reichelstein, 2010, 2021).

Public debates about regulating carbon emissions often center on how alternative policy instruments affect the production costs of essential goods and services. Our model allows analysts to quantify the *Levelized Cost per Mile* (LCM) of the vehicle fleet under different policy instruments and emission targets.[15] Let η_i denote the average energy efficiency (in

[15]Levelized cost measures have been widely examined in the energy economics literature (see, for instance, Joskow (2011); Glenk and Reichelstein (2022)). In a generic model, Reichelstein and Rohlfing-Bastian (2015) argue that the levelized product cost represents the long-run marginal product cost, since the expected market price in a competitive market equilibrium must equal the levelized product cost.

miles per kWh) of the electric drivetrain of vehicle i. Suppose the firm expects a future emission charge of p that incentivizes annual emissions $E^*(p)$ and electric capacity $c_i^{e*}(E^*(p))$ for each vehicle i. The fleet's levelized cost per mile is then given by the total cost of fleet ownership and emissions compliance, divided by the life-cycle miles driven. Formally:

$$LCM(E^*(p)|p) \equiv \frac{\sum_{i=1}^{n} TCO_i(c_i^{e*}(E^*(p))) + p \cdot E^*(p) \cdot A(\delta, T)}{A(\delta, T) \cdot \sum_{i=1}^{n} \sum_{j=1}^{m} \eta_i \cdot r_{ij}}. \tag{13}$$

Current emission charges often provide only limited incentives for firms to decarbonize. To accelerate the adoption of low-emission drivetrains, regulators in California, the European Union, and other jurisdictions have introduced emission performance standards for newly registered vehicles across vehicle classes.[16] The following result quantifies the resulting increase in the fleet's levelized cost per mile when the firm anticipates an emission charge p that induces annual emissions $E^*(p)$ but is also required to meet an emission target $E^+ < E^*(p)$.

Proposition 5. *Suppose the firm expects an emission charge p in the future that incentivizes annual emissions of $E^*(p)$ but is also required to meet an emission target $E^+ < E^*(p)$. The corresponding change in the levelized cost per mile of the vehicle fleet is then given by:*

$$\Delta LCM(E^+|p) = \frac{TAC(E^+|E^*(p)) - p \cdot (E^*(p) - E^+) \cdot A(\delta, T)}{A(\delta, T) \cdot \sum_{i=1}^{n} \sum_{j=1}^{m} \eta_i \cdot r_{ij}}.$$

The expression in Proposition 5 follows directly from taking the difference between $LCM(E^+|p)$ and $LCM(E^*(p)|p)$ in equation (13). It reflects the increase in the product price required to make the firm indifferent between emitting $E^*(p)$ annually and further decarbonizing the vehicle fleet to limit annual emissions to E^+. When the target E^+ arises from a voluntary climate pledge rather than a direct mandate, this price increment reflects the "green premium" the firm would need to charge to its customers for transportation services with lower carbon footprints. This premium can be viewed as an indicator of both the ambition and the credibility of a firm's climate commitment.[17]

Rather than imposing emission performance standards, regulators could also increase the emission charges, for example, by tightening the emissions cap or raising the minimum price for emission permits in cap-and-trade systems.[18] The following result quantifies the resulting

[16] California requires public transit agencies to only procure zero-emission buses from 2029 (CARB, 2018).

[17] See Bolton and Kacperczyk (2025); Jiang et al. (2025); Comello et al. (2022) for recent evaluations of the credibility and ambition of corporate climate commitments.

[18] In California, emission caps decline while minimum auction prices for emission permits rise each year

increase in the fleet's levelized cost per mile when further decarbonization is driven by higher carbon prices.

Corollary to Proposition 5. *Suppose the firm reduces its annual emissions from $E^*(p)$ to $E^*(p^+)$ in response to an increase in the expected emission charge from p to p^+. The corresponding change in the levelized cost per mile of the vehicle fleet is then given by:*

$$\Delta LCM(p^+|p) = \Delta LCM(E^*(p^+)|p) + \frac{E^*(p^+) \cdot (p^+ - p)}{\sum_{i=1}^{n} \sum_{j=1}^{m} \eta_i \cdot r_{ij}}.$$

The cost metrics, $\Delta LCM(E^+|p)$ and $\Delta LCM(p^+|p)$, respectively capture the firm's private compliance cost when additional abatement is induced by either a mandate to lower emissions E^+ or higher carbon prices p^+. Both metrics include resource cost in the form of the incremental total abatement cost resulting from technological and operational changes required to reduce emissions. When $E^+ = E^*(p^+)$, this cost component is identical under the two policy instruments, since both induce the same fleet configuration.

As the preceding Corollary shows, $\Delta LCM(p^+|p)$ also includes the additional charges on residual emissions (i.e., $E^*(p^+) \cdot (p^+ - p)$) the firm incurs as a result of higher carbon prices. Importantly, the magnitude of these additional charges depends on the elasticity of the firm's optimal emission response to carbon prices. When this response is inelastic (elastic), annual emissions fall slowly (rapidly), and the additional charges on residual emissions are large (small).

We further note that payments for emission charges reflect transfers to the regulator. The regulator may, in turn, use these transfers, for example, to support the adoption of electric drivetrains. Such support would lower the firm's private incremental total abatement cost of reaching the lower emission level and thereby narrow the gap between $\Delta LCM(E^+|p)$ and $\Delta LCM(p^+|p)$.

4.2 Application to Urban Bus Fleets

Figure 5 shows the optimal emission response of urban bus fleets to different carbon prices. We find that this response is fairly inelastic, especially at low and high prices. Emission permits under California's Cap-and-Trade Program traded at an average of \$35/tCO_2e in 2024 (ICAP, 2025). At this price, firms are incentivized to expand electric capacity across

(ICAP, 2025).

vehicles such that they constitute 70% of usable installed capacity and 92% of annual demand. Annual emissions would fall to 377 tCO_2e (69% of E_0). Despite this reduction, a 1.0% increase in carbon prices would induce further emission reductions of only about 0.55%. Above an abatement of about 90%, the price elasticity of abatement approaches zero. If deep decarbonization of urban bus fleets is to be induced by emission charges, these charges would have to rise exponentially to several hundred dollars per ton of CO_2e.

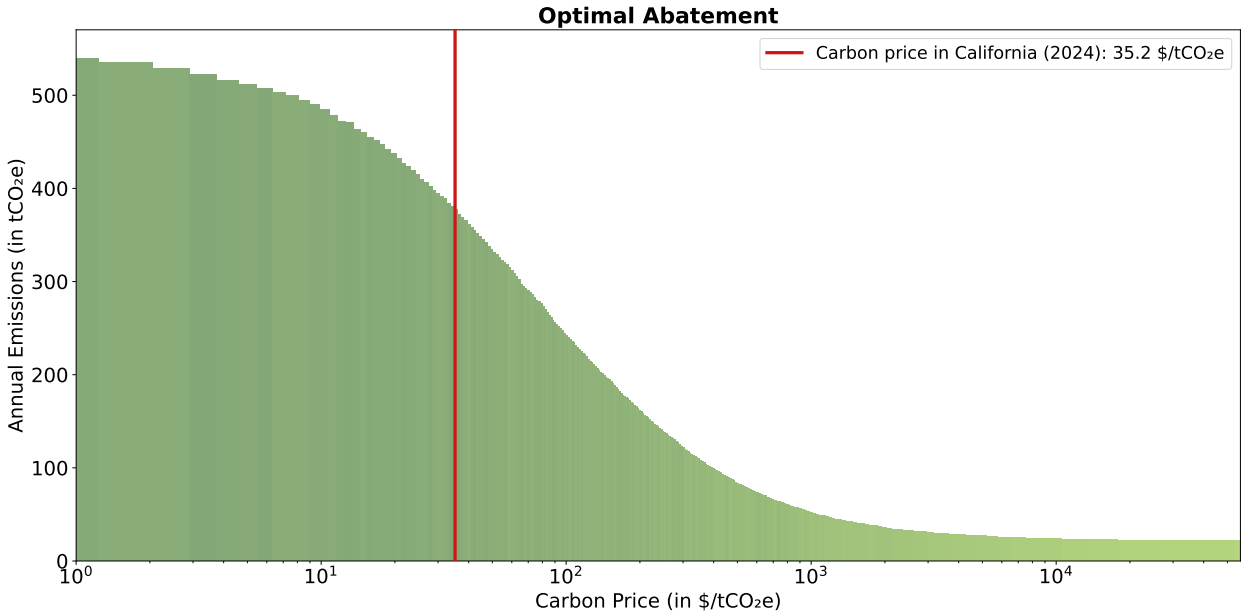


Figure 5. Optimal abatement of urban buses. This figure shows the optimal emission response to different carbon prices.

Figure 6a shows the resulting increase in the levelized cost per mile of urban bus fleets, $\Delta LCM(E^+|p)$, when urban bus fleets are required to reduce emissions to some target E^+, while the prevailing carbon price of p only incentivizes an optimal emissions level of $E^*(p)$. To illustrate our findings, suppose that firms expect a carbon price of \$35/tCO_2e to persist and therefore reduce their annual emissions to $E^*(35) = 377$ tCO_2e (69% of E_0). The red line in Figure 6a shows that if firms are required to reduce emissions all the way to $E_- = 21.95$ tCO_2e (4% of E_0), the levelized cost increases by only ¢7.5 per mile, or 2.4% relative to the case where the firms stay at $E^*(35) = 377$ tCO_2e.

Alternatively, Figure 6b shows the increase in the levelized cost per mile, $\Delta LCM(p^+|p)$, if the prevailing carbon price increases from p to p^+. Suppose that firms again anticipate a carbon price of \$35/tCO_2e and therefore reduce their annual emissions to $E^*(35) = 377$ tCO_2e (69% of E_0). If the carbon price were to rise sufficiently to induce emission reductions

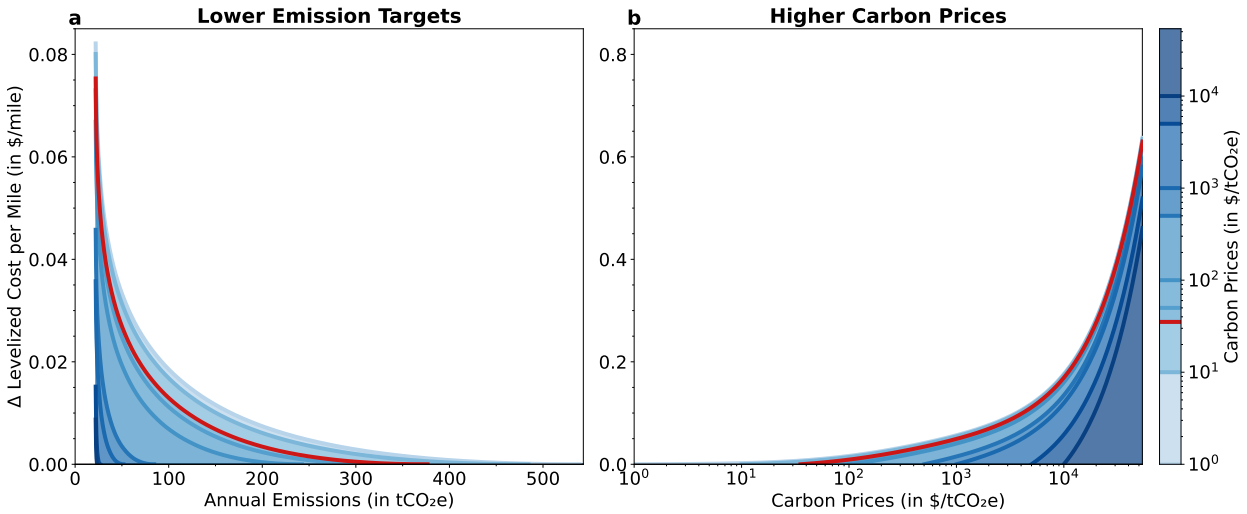


Figure 6. Change in the levelized cost per mile of urban buses. This figure shows (**a**) the resulting change in the levelized cost per mile, $\Delta LCM(E^+|p)$, when firms seek to reduce emissions from $E^*(p)$ to some target E^+ and (**b**) the resulting change in the levelized cost per mile, $\Delta LCM(p^+|p)$, when the prevailing carbon price increases from p to p^+.

to 54 tCO_2e (about 10% of E_0), the levelized cost depicted by the red line would increase by ¢4.8 per mile, or 1.5% relative to the case without higher prices. If carbon prices were to rise even further to induce maximal decarbonization to $E_- = 21.95$ tCO_2e, the levelized cost would increase by ¢63 per mile, or 19.9% relative to the case without higher prices.[19]

Consistent with our analytical characterization, the increase in the levelized cost per mile for a given emission target, E^+, is higher when the target is driven by carbon prices rather than regulatory mandates or voluntary pledges. In our example, the difference is particularly pronounced (i.e., $\$0.63 - 0.075$ per mile) because of the low price elasticity of abatement (note that the y-axis in Figure 6b spans 10 times the range in Figure 6a). These findings support the view that carbon pricing and emission performance standards, as adopted together in California, the European Union, and other jurisdictions, are complementary policy instruments for achieving deep decarbonization of vehicle fleets (Stechemesser et al., 2024).

5 Discussion

Our base model has treated drivetrain capacity as a continuous choice with additive costs across the two drivetrains. When drivetrain capacity is discrete, as is typically the case in

[19] In comparison, the minimum auction price for emission permits in California was about $\$24/tCO_2e$ in 2024 and is scheduled to increase annually by 5% plus inflation (ICAP, 2025).

practice, firms will seek to choose the available sizes closest to the cost-efficient ones identified in our results. When installing a drivetrain also entails a fixed cost for its power component, firms will further choose among pure diesel, fully electric, and hybrid configurations for each vehicle, as shown in Appendix A4. In that case, the cost-efficient fleet will likely include fewer hybrids as vehicles with a high (low) share of electric capacity will shift toward fully electric (pure diesel) drivetrains. Both extensions should yield vehicle configurations where electric drivetrains serve shares of annual demand close to those in our main results, while modestly increasing the costs of decarbonizing urban bus fleets.

Our numerical analysis has relied on point estimates of cost parameters, as reported in Table 1. These point estimates are based on arithmetic means of cost estimates obtained via comprehensive reviews (see Appendix A2 for details). The variation among these estimates indicates uncertainty where the actual probability distributions have yet to be observed. Regardless of these distributions, the total cost of ownership and corresponding abatement costs in Figure 3 can be interpreted as the expected costs derived from a model with cost uncertainty, provided that the expected value of each cost parameter is equal to its arithmetic mean, as noted in Section 2.1. To further examine variation in cost parameters, we test the sensitivity of our results to small simultaneous deviations in the cost estimates. This analysis, detailed in Appendix A3, delivers a fairly robust assessment of the cost-efficient configuration and the total abatement costs of urban bus fleets today.

With electric vehicle adoption accelerating, battery technology is expected to improve in cost and energy density as learning effects continue to materialize. At the same time, some voices in recent policy debates have argued that vehicles with internal combustion engines could achieve lower life-cycle net emissions by using low-emission fuels. We examine the impact of both possibilities in Appendix A3 based on estimates of the corresponding parameters expected to materialize over the coming years. Our calculations project that both possibilities increase the electric capacity across vehicles in the cost-efficient fleet and reduce the total abatement costs. In particular, if battery technology improves as expected over the coming years (Link et al., 2024), then (near) complete decarbonization of urban bus fleets would entail an estimated annualized total abatement cost of \$113,826–157,696, or 1.7–2.4% of the estimated annualized total cost of ownership for the cost-efficient fleet. Yet, the optimal emission response to carbon prices remains fairly inelastic, meaning that policy mixes combining carbon pricing with emission performance standards remain effective.

Overall, our findings are corroborated by the recent surge in the global adoption of electric transit buses (IEA, 2025b). Relative to recent studies, our estimates of the cost of decarbonizing vehicle fleets are more detailed and generally more favorable.[20] These differences reflect the more recent industry data that capture improvements in the cost and performance of electric drivetrains. They also reflect our embedded optimization algorithm, which determines the cost-efficient capacity and deployment of electric and diesel drivetrains for each abatement target. If firms instead did not deploy alternative drivetrains cost-efficiently due to neglect or operational constraints, Appendix A3 shows that the electric capacity in the cost-efficient fleet would be substantially lower than in Figure 2, while the total abatement costs would be substantially higher than in Figure 3 for any given target.

Beyond urban buses, our model is directly applicable to other vehicle fleets. As detailed in Appendix A5, fleets with regular duty cycles anchored at central depots (e.g., delivery vans and trucks, municipal and (air)port vehicles, and local ferries) typically exhibit fairly uniform load duration curves with occasional moderate peaks. Accordingly, they are set to exhibit high shares of electric capacity in the cost-efficient configuration and to achieve deep decarbonization at modest cost. In contrast, heavy-duty fleets operating multi-leg rotations (e.g., long-haul trucks, cargo ships, and commercial airplanes) face consistently high energy demand on most days. Such fleets will likely continue to rely primarily on conventional drivetrains for the cost-efficient configuration in the near term. Yet, rapid advances in battery technology, expansions of fast-charging infrastructure, and the development of new propulsion systems suggest that this pattern may soon change.

We also argue that our model can be adapted to other industries with multiple operating assets. For example, technology companies can adapt our model to assess the costs of deploying renewable energy and storage across data centers worldwide, accounting for local and temporal variations in computing demand and the availability of renewable power. Similarly, companies with multiple offices, retail sites, or production facilities can adapt our model to coordinate investments in renewable power and heat pumps across locations based on local variations in the emission intensity of electricity grids and the costs of renewable energy.[21]

[20] See, for instance, Comello et al. (2021); Harris et al. (2020); Gunawan and Monaghan (2022); Lajunen and Lipman (2016).

[21] For example, Apple (2024), Google (2025), and Microsoft (2025) have installed wind and solar energy sources near their data centers. German grocery chains, such as Aldi (2025) and Lidl (2022), are similarly installing rooftop solar systems across their stores worldwide.

6 Concluding Remarks

This paper has introduced an abatement cost model that enables firms to assess the costs of technological and operational changes required across operating assets to achieve firm-wide emission reductions. We calibrate our model with new industry data in the context of urban bus fleets regulated under the California Cap-and-Trade Program. We find that a carbon price of \$35/tCO_2e, the 2024 average, incentivizes firms to configure their fleets such that battery-electric drivetrains constitute 70% of usable installed capacity and 92% of annual demand, while diesel drivetrains mainly serve occasional peaks. Yet, this incentive is highly inelastic, meaning that further reductions in diesel capacity require emission charges that would sharply increase the levelized cost per mile of the fleets. If firms were instead mandated to further phase down diesel capacity, the levelized cost per mile would rise by at most 2.4%.

Future research could model electric vehicle adoption as a dynamic capacity replacement problem under uncertainty. In practice, fleet operators may gradually replace vehicles as they reach the end of their useful life or their continued operation becomes more costly than the adoption of new vehicles with electric drivetrains. Battery technology is further expected to improve in cost and energy density at uncertain rates, while carbon prices in cap-and-trade programs are volatile and expected to rise as emission caps tighten. Incorporating such uncertainties in a dynamic program would allow firms to quantify the option value of waiting for particular technology and market developments before committing irreversible investments (Falbo et al., 2021).

It would also be insightful to examine the cost implications of emerging technologies such as hydrogen-electric drivetrains or opportunity charging for battery-electric drivetrains. Hydrogen-electric drivetrains could replace diesel drivetrains as peaker capacity, enabling firms to achieve zero direct emissions. Opportunity charging, i.e., brief charging boosts during operation, could extend the effective daily range of electric drivetrains and thereby allow for lower electric capacity. Both advances could significantly reduce the cost of decarbonizing vehicle fleets, especially in heavy-duty applications.

Appendix

A1 Proofs

Lemma 1

Given feasible drivetrain capacity sizes, the objective is:

$$\min_{\substack{\vec{x}\in X\\ \vec{q}\in Q}}\left\{\sum_{k=1}^{n}\sum_{i=1}^{n}\sum_{j=1}^{m} x_{ijk}\cdot\left[(q^e_{ijk}+q^d_{ijk})\cdot w + q^e_{ijk}\cdot w^e + q^d_{ijk}\cdot w^d\right]\right\}. \tag{A1}$$

Since $w^e < w^d$, it is cost-efficient for the firm to use the electric drivetrain of each vehicle k first on any assigned daily route r_{ij}. Thus, $q^{e*}_{ijk} = \min\{r_{ij}, c^e_k\}$ and $q^{d*}_{ijk} = \big(r_{ij} - \min\{r_{ij}, c^e_k\}\big)$. Inserting q^{e*}_{ijk} and q^{d*}_{ijk} in equation (A1) and rearranging the resulting expression yields:

$$\min_{\vec{x}\in X}\left\{(w+w^d)\cdot\sum_{i=1}^{n}\sum_{j=1}^{m} r_{ij} - (w^d-w^e)\cdot\sum_{k=1}^{n}\sum_{i=1}^{n}\sum_{j=1}^{m} x_{ijk}\cdot\min\{r_{ij}, c^e_k\}\right\},$$

which is equivalent to:

$$\min_{\vec{x}\in X}\left\{\sum_{i=1}^{n}\sum_{k=1}^{n} x_{ijk}\cdot\big(-\min\{r_{ij}, c^e_k\}\big)\right\}, \tag{A2}$$

on each day j, provided that vehicle-to-route assignments are separable across days.

The expression in equation (A2) reflects a standard linear sum assignment problem, where the terms $(-\min\{r_{ij}, c^e_k\})$ form the elements of an $n \times n$ "cost" matrix. As described on pages 151–152 of the textbook by Burkard et al. (2009), an $n \times n$ cost matrix C is a so-called *Monge* matrix if its elements $c_{ij} = \min\{a_i, b_j\}$ for increasing real numbers $a_i \leq \ldots \leq a_n$ and decreasing real numbers $b_i \geq \ldots \geq b_n$. Every Monge matrix satisfies the *weak Monge property* that $c_{ii} + c_{kl} \leq c_{il} + c_{ki}$ for $1 \leq i < k \leq n$ and $1 \leq i < l \leq n$. By Proposition 5.7 of the textbook, a linear sum assignment problem whose cost matrix is a weak Monge matrix is solved by the identical permutation, i.e., the assignment variable $x_{ij} = 1$ if and only if $i = j$ and zero otherwise.

Returning to our analysis, recall that vehicles and daily routes are sorted and indexed so that $c^e_1 \geq \ldots \geq c^e_n$ and $r_{1j} \geq \ldots \geq r_{nj}$ for each day j. By Burkard et al. (1996), the $n \times n$ matrix with elements $(-\min\{r_{ij}, c^e_k\})$ is an inverse Monge matrix, i.e., a Monge matrix. The expression in equation (A2) is therefore solved by setting $x_{ijk} = 1$ if and only if $i = k$ and zero otherwise, thus establishing Lemma 1. □

Lemma 2

As stated in Section 2.1, the term $\min\{r_{ij}, c_i^e\}$ is piecewise linear and concave in c_i^e. Summing over days j preserves these properties. Multiplication by the negative coefficient makes the resulting function convex. □

Proposition 1

Since $TCO_i(\cdot)$ is piecewise linear, its minimum will be achieved at one of the breakpoints $\{0, r_i^{m_i^+}, r_i^{m_i^+-1}, \ldots, r_i^1\}$ or $\bar{c}_i^e$. Suppose now that $u-1 \leq \lambda_i \leq u \leq m_i^+$ and $r_i^u \leq \bar{c}_i^e$. By the convexity of $TCO_i(\cdot)$, it suffices to show that $TCO_i(r_i^u) \leq TCO_i(r_i^{u-1})$ and $TCO_i(r_i^u) \leq TCO_i(r_i^{u+1})$. To verify that $TCO_i(r_i^u) \leq TCO_i(r_i^{u-1})$, we write

$$TCO_i(r_i^u) = a_i + X_i \cdot r_i^u - Y \cdot \left[\sum_{j=1}^{u} r_i^u + \sum_{j=u+1}^{m_i^+} r_i^j\right],$$

where $X_i \equiv v_i^e - v_i^d$ and $Y \equiv A(\delta, T) \cdot (w^d - w^e)$. Thus

$$\begin{aligned} TCO_i(r_i^u) - TCO_i(r_i^{u-1}) &= X_i \cdot (r_i^u - r_i^{u-1}) - Y \cdot \left[\sum_{j=1}^{u} r_i^u - \left(\sum_{j=1}^{u-1} r_i^{u-1} + r_i^u\right)\right] \\ &= X_i \cdot (r_i^u - r_i^{u-1}) - Y \cdot (u-1) \cdot (r_i^u - r_i^{u-1}) \\ &= (r_i^u - r_i^{u-1}) \cdot \big[X_i - Y \cdot (u-1)\big]. \end{aligned}$$

This expression is less than or equal to zero if and only if $X_i - Y \cdot (u-1) \geq 0$, which is equivalent to $\lambda_i \geq u-1$. If $r_i^{u-1} \geq \bar{c}_i^e$, the same sequence of steps shows that $TCO_i(r_i^u) \leq TCO(\bar{c}_i^e)$. Finally, the inequality $TCO_i(r_i^u) \leq TCO_i(r_i^{u+1})$ follows in direct analogy to the preceding steps after observing that $\lambda_i \leq u$. □

Proposition 2

Let $V(E) \equiv \min_{\vec{c} \in C(E)} \sum_{i=1}^n TCO_i(c_i^e)$. By the argument in the proof to Lemma 2, the objective $\sum_{i=1}^n TCO_i(\cdot)$ and the constraint $\sum_{i=1}^n E_i(\cdot) \leq E$ are each piecewise linear and convex in c_i^e. Since a sublevel set of a convex function is convex, the feasible set $C(E)$ is convex in $\vec{c}$.

Minimizing a piecewise linear objective subject to a piecewise linear constraint yields a piecewise linear minimum-value function. To see this, we formulate the cost minimization as an equivalent linear program. Introduce auxiliary variables $y_{ij} \in [0, r_{ij}]$ with $y_{ij} \leq c_i^e$, so that $\min\{r_{ij}, c_i^e\} = y_{ij}$ in the optimum and $\sum_{j=1}^m \min\{r_{ij}, c_i^e\} = \sum_{j=1}^m y_{ij}$. By Lemma 2, $TCO_i(\cdot)$

is convex and piecewise linear with breakpoints $\{r_i^0, r_i^1, \ldots, r_i^{m_i^+}, r_i^{m_i^+ +1}\}$, where we set $r_i^0 \equiv \bar{c}_i^e$ and $r_i^{m_i^+ +1} \equiv 0$ for notational simplicity. Let $\alpha_{iu} \equiv MCO_i(r_i^u)$ for $u = 0, \ldots, m_i^+$ capture the slope of the $TCO_i(\cdot)$ function on the interval $[r_i^{u+1}, r_i^u]$. Let also $\beta_{iu} \equiv TCO_i(r_i^{u+1}) - \alpha_{iu} \cdot r_i^{u+1}$ for $u = 0, \ldots, m_i^+$ capture the corresponding intercept, where $TCO_i(r_i^{u+1})$ can be determined recursively as

$$TCO_i(r_i^{u+1}) = TCO_i(0) + \sum_{v=u+1}^{m_i^+} \alpha_{iv} \cdot (r_i^v - r_i^{v+1}),$$

for $u = 0, \ldots, m_i^+$. Thus, for all $c_i^e \in [0, \bar{c}_i^e]$,

$$TCO_i(c_i^e) = \max_{u=0,\ldots,m_i^+} \{\alpha_{iu} \cdot c_i^e + \beta_{iu}\}.$$

With the epigraph variables t_i, the function $V(E) = \min_{\vec{c} \in C(E)} \sum_{i=1}^n TCO_i(c_i^e)$ is equivalent to the (polyhedral) linear program:

$$\begin{array}{lll}
\min\limits_{\{c_i^e\},\{y_{ij}\},\{t_i\}} & \sum\limits_{i=1}^n t_i & \\
\text{subject to} & t_i \geq \alpha_{iu} \cdot c_i^e + \beta_{iu}, & i = 1, \ldots, n,\ u = 0, \ldots, m_i^+, \\
& \sum\limits_{i=1}^n \sum\limits_{j=1}^m (r_{ij} - y_{ij}) \cdot \theta \leq E, & \\
& 0 \leq c_i^e \leq \bar{c}_i^e, & i = 1, \ldots, n, \\
& 0 \leq y_{ij} \leq r_{ij}, & i = 1, \ldots, n,\ j = 1, \ldots, m, \\
& y_{ij} \leq c_i^e, & i = 1, \ldots, n,\ j = 1, \ldots, m.
\end{array}$$

In this formulation, the target E enters only through the right-hand-side of the emission constraint. Since the optimal value of a linear program as a function of a right-hand-side parameter is piecewise affine, the minimum-value function $V(\cdot)$ is piecewise linear in E.

Minimizing a convex objective over a convex set yields a convex minimum-value function. To see this, suppose $\{c_i^{e*}(E_1)\}_{i=1}^n$ and $\{c_i^{e*}(E_2)\}_{i=1}^n$ minimize $TAC(E_1|E_0)$ and $TAC(E_2|E_0)$, respectively. Suppose further that $E = \omega \cdot E_1 + (1-\omega) \cdot E_2$. We first verify that $\{\omega \cdot c_i^{e*}(E_1) + (1-\omega) \cdot c_i^{e*}(E_2)\}_{i=1}^n$ is feasible if the abatement target is E. This follows from the convexity

of the functions $E_i(\cdot)$ as:

$$\begin{aligned}
&\sum_{i=1}^{n} E_i\big(\omega \cdot c_i^{e*}(E_1) + (1-\omega) \cdot c_i^{e*}(E_2)\big) \\
&\leq \omega \cdot \sum_{i=1}^{n} E_i\big(c_i^{e*}(E_1)\big) + (1-\omega) \cdot \sum_{i=1}^{n} E_i\big(c_i^{e*}(E_2)\big) \\
&\leq \omega \cdot E_1 + (1-\omega) \cdot E_2 \\
&= E.
\end{aligned}$$

Similarly, regarding the objective function, we observe that

$$V\big(\omega \cdot E_1 + (1-\omega)E_2\big) \leq \sum_{i=1}^{n} TCO_i\big(\omega \cdot c_i^{e*}(E_1) + (1-\omega) \cdot c_i^{e*}(E_2)\big),$$

provided $\{\omega \cdot c_i^{e*}(E_1) + (1-\omega) \cdot c_i^{e*}(E_2)\}_{i=1}^{n}$ is feasible for target level E. But

$$\begin{aligned}
&\sum_{i=1}^{n} TCO_i\big(\omega \cdot c_i^{e*}(E_1) + (1-\omega) \cdot c_i^{e*}(E_2)\big) \\
&\leq \omega \cdot \sum_{i=1}^{n} TCO_i\big(c_i^{e*}(E_1)\big) + (1-\omega) \cdot \sum_{i=1}^{n} TCO_i\big(c_i^{e*}(E_2)\big) \\
&= \omega \cdot V(E_1) + (1-\omega) \cdot V(E_2).
\end{aligned}$$

Considering these inequalities yields the claim. □

Lemma 3

By the proof to Proposition 2, minimizing $\sum_{i=1}^{n} TCO_i(c_i^e)$ subject to $\sum_{i=1}^{n} E_i(c_i^e) \leq E$ can be formulated as an equivalent linear program. This program is feasible by construction for any emission target $E \in [E_-, E_0]$. Its optimal value is finite because the variables c_i^e and y_{ij} are bounded, and each epigraph variable t_i is bounded below by finitely many affine functions over a bounded domain. With the base set reflecting the entire space of decision variables, the program also has a feasible point in the relative interior of this base set.

Thus, Corollary 28.2.2 in Rockafellar (1997) implies the existence of a Kuhn–Tucker vector for the full constraint system. Let $\mu \geq 0$ denote the component of such a vector corresponding to the emission constraint. Corollary 28.3.1 (Kuhn-Tucker Theorem) in Rockafellar (1997) further implies that an optimal solution to the linear program can be obtained by minimizing the corresponding Lagrangian over all choice variables of the linear program. That is, these

optimal variables of the linear program, together with the Kuhn-Tucker vector, form a saddle point of the Lagrangian.

To characterize the multiplier $\mu \geq 0$ corresponding to setting the emission constraint to E, let $V(E) = \min_{\vec{c} \in C(E)} \sum_{i=1}^{n} TCO_i(c_i^e)$. By the saddle-point property, it holds for any $E, E' \in [E_-, E_0]$:

$$\begin{aligned} V(E) &\leq \sum_{i=1}^{n} TCO_i(c_i^e) + \mu \cdot \Big(\sum_{i=1}^{n} E_i(c_i^e) - E \Big) \\ &\leq \sum_{i=1}^{n} TCO_i(c_i^e) + \mu \cdot \Big(E' - E \Big) \end{aligned}$$

Minimizing $\sum_{i=1}^{n} TCO_i(c_i^e)$ over $\vec{c} \in C(E')$ yields:

$$V(E') \geq V(E) - \mu \cdot (E' - E),$$

so $-\mu$ reflects a subgradient of $V(\cdot)$ at E.

Recall from the proof to Proposition 2 that $V(\cdot)$ is piecewise linear and convex in E. On any open interval between two consecutive breakpoints, $V(\cdot)$ is affine and hence differentiable, so the multiplier μ is unique and equals the negative slope of V on that interval. Formally, on (E_k, E_{k-1}):

$$\mu \;=\; \frac{V(E_k) - V(E_{k-1})}{E_{k-1} - E_k} \;=\; \frac{TAC(E_k \mid E_{k-1})}{E_{k-1} - E_k} \;=\; MAC(E_k) \cdot A(\delta, T).$$

At a breakpoint E_k, $V(\cdot)$ is generally not differentiable. Theorem 23.2 in Rockafellar (1997) implies that, for a one-dimensional convex function, the subgradient at such a point is the closed interval between the left and right derivatives. Hence the multiplier μ can take any value in the corresponding interval of slopes, which in our notation implies, for $k = 1, \ldots, s-1$,

$$MAC(E_{k+1}) \cdot A(\delta, T) \;\geq\; \mu \;\geq\; MAC(E_k) \cdot A(\delta, T),$$

while $\mu \geq MAC(E_s) \cdot A(\delta, T)$. At E_0, the emissions constraint does not change at the unconstrained cost minimum and thus $\mu = 0$. Since μ is not unique at a breakpoint, we denote by $\mu(E_k) = MAC(E_k) \cdot A(\delta, T)$ the tie-breaking choice corresponding to the linear segment of the $TAC(\,\cdot\,|E_0)$ curve ending at E_k. □

Proposition 3

Given an emission target E_k, the firm's objective is to choose c_i^e for each vehicle i so as to minimize:

$$Z_i(c_i^e) \equiv TCO_i(c_i^e) + \mu(E_k) \cdot E_i(c_i^e).$$

Let $\mu^*(E_k) \geq 0$ denote an optimal Lagrange multiplier corresponding to setting the emission constraint to E_k. By Lemma 2 and the arguments in the proof to Proposition 2, the function $Z_i(\cdot)$ is piecewise linear and convex in c_i^e. Thus, its minimum will be achieved at one of the breakpoints $\{0, r_i^{m_i^+}, r_i^{m_i^+-1}, \ldots, r_i^1\}$ or $\bar{c}_i^e$.

In direct analogy to the proof to Proposition 1, suppose that $u-1 \leq \lambda_i(E_k) \leq u \leq m_i^+$ and $r_i^u \leq \bar{c}_i^e$. By the convexity of $Z_i(\cdot)$, it suffices to show that $Z_i(r_i^u) \leq Z_i(r_i^{u-1})$ and $Z_i(r_i^u) \leq Z_i(r_i^{u+1})$. To verify that $Z_i(r_i^u) \leq Z_i(r_i^{u-1})$, we write

$$Z_i(r_i^u) = a_i + X_i \cdot r_i^u - Y \cdot \left[\sum_{j=1}^{u} r_i^u + \sum_{j=u+1}^{m_i^+} r_i^j\right] + \mu^*(E_k) \cdot \theta \cdot \left[\sum_{j=1}^{m_i^+} r_i^j - \left(\sum_{j=1}^{u} r_i^u + \sum_{j=u+1}^{m_i^+} r_i^j\right)\right],$$

where $X_i \equiv v_i^e - v_i^d$ and $Y \equiv A(\delta, T) \cdot (w^d - w^e)$. Thus,

$$\begin{aligned} Z_i(r_i^u) - Z_i(r_i^{u-1}) &= X_i \cdot (r_i^u - r_i^{u-1}) - \big(Y + \mu^*(E_k) \cdot \theta\big) \cdot \left[\sum_{j=1}^{u} r_i^u - \left(\sum_{j=1}^{u-1} r_i^{u-1} + r_i^u\right)\right] \\ &= X_i \cdot (r_i^u - r_i^{u-1}) - \big(Y + \mu^*(E_k) \cdot \theta\big) \cdot (u-1) \cdot (r_i^u - r_i^{u-1}) \\ &= (r_i^u - r_i^{u-1})\Big[X_i - \big(Y + \mu^*(E_k) \cdot \theta\big) \cdot (u-1)\Big]. \end{aligned}$$

This expression is less than or equal to zero if and only if $X_i - \big(Y + \mu^*(E_k) \cdot \theta\big) \cdot (u-1) \geq 0$, which is equivalent to $\lambda_i(E_k) \geq u-1$. If $r_i^{u-1} \geq \bar{c}_i^e$, the same sequence of steps shows that $Z_i(r_i^u) \leq Z_i(\bar{c}_i^e)$. Finally, the inequality $Z_i(r_i^u) \leq Z_i(r_i^{u+1})$ follows in direct analogy to the preceding steps after observing that $\lambda_i(E_k) \leq u$. □

Proposition 4

By Proposition 2, the $TAC(\cdot|E_0)$ function is piecewise linear and convex in E with breakpoints $E_- = E_s < \cdots < E_0$. The function

$$Z(E, p|E_0) \equiv TAC(E|E_0) - p \cdot (E_0 - E) \cdot A(\delta, T)$$

adds an affine term in E. Affine transformations preserve both piecewise linearity and

convexity and do not introduce additional breakpoints. Thus $Z(\cdot, p|E_0)$ is piecewise linear and convex in E with the same breakpoints $E_- = E_s < \cdots < E_0$. The minimum of the $Z(\cdot, p|E_0)$ function will therefore be achieved at one of the breakpoints or on the entire segment between two breakpoints and, it suffices to show that $Z(E_k, p|E_0) \leq Z(E_{k-1}, p|E_0)$ and $Z(E_k, p|E_0) \leq Z(E_{k+1}, p|E_0)$. Thus,

$$\begin{aligned} Z(E_k, p|E_0) - Z(E_{k-1}, p|E_0) &= TAC(E_k|E_0) - p \cdot (E_0 - E_k) \cdot A(\delta, T) \\ &\quad - TAC(E_{k-1}|E_0) + p \cdot (E_0 - E_{k-1}) \cdot A(\delta, T) \\ &= TAC(E_k|E_{k-1}) - p \cdot (E_{k-1} - E_k) \cdot A(\delta, T). \end{aligned}$$

This expression is less than or equal to zero if and only if $p \geq MAC(E_k)$. The inequality $Z(E_k, p|E_0) \leq Z(E_{k+1}, p|E_0)$ follows in direct analogy to the preceding steps after observing that $p \leq MAC(E_{k+1})$. If $p = MAC(E_k)$, any emission level on the interval $[E_k, E_{k-1}]$ is optimal. Adopting the tie-breaking convention that the firm selects the lowest emission level if multiple levels are optimal, we obtain that $E^*(p) = E_k$ if and only if $MAC(E_{k+1}) > p \geq MAC(E_k)$. Boundary cases follow directly: $E^*(p) = E_0$ if and only if $MAC(E_1) > p$, while $E^*(p) = E_s$ if and only if $p \geq MAC(E_s)$. □

Proposition 5

Suppose the firm expects an emission charge p in the future that incentivizes annual emissions $E^*(p)$ but is also required to meet an emission target $E^+ < E^*(p)$. The corresponding increase in the levelized cost per mile of the vehicle fleet follows directly from taking the difference between $LCM(E^+|p)$ and $LCM(E^*(p)|p)$ in equation (13). Thus:

$$\begin{aligned} &LCM(E^+|p) - LCM(E^*(p)|p) \\ &= \frac{\sum_{i=1}^{n} TCO_i(c_i^{e*}(E^+)) - \sum_{i=1}^{n} TCO_i(c_i^{e*}(E^*(p))) - p \cdot (E^*(p) - E^+) \cdot A(\delta, T)}{A(\delta, T) \cdot \sum_{i=1}^{n} \sum_{j=1}^{m} \eta_i \cdot r_{ij}} \\ &= \frac{TAC(E^+|E^*(p)) - p \cdot (E^*(p) - E^+) \cdot A(\delta, T)}{A(\delta, T) \cdot \sum_{i=1}^{n} \sum_{j=1}^{m} \eta_i \cdot r_{ij}} \\ &= \Delta LCM(E^+|p) \end{aligned}$$

□

Corollary to Proposition 5

Suppose the firm reduces its annual emissions from $E^*(p)$ to $E^*(p^+)$ in response to an increase

in the expected emission charge from p to p^+. The corresponding change in the levelized cost per mile of the vehicle fleet follows again from taking the difference between $LCM(E^*(p^+)|p)$ and $LCM(E^*(p)|p)$ in equation (13). Thus:

$$
\begin{aligned}
&LCM(E^*(p^+)|p) - LCM(E^*(p)|p) \\
&= \frac{\sum_{i=1}^{n} TCO_i(c_i^{e*}(E^*(p^+))) - \sum_{i=1}^{n} TCO_i(c_i^{e*}(E^*(p))) + [p^+ \cdot E^*(p^+) - p \cdot E^*(p)] \cdot A(\delta, T)}{A(\delta, T) \cdot \sum_{i=1}^{n} \sum_{j=1}^{m} \eta_i \cdot r_{ij}} \\
&= \frac{TAC(E^*(p^+)|E^*(p)) - [p \cdot (E^*(p) - E^*(p^+)) - E^*(p^+) \cdot (p^+ - p)] \cdot A(\delta, T)}{A(\delta, T) \cdot \sum_{i=1}^{n} \sum_{j=1}^{m} \eta_i \cdot r_{ij}} \\
&= \Delta LCM(E^*(p^+)|p) + \frac{E^*(p^+) \cdot (p^+ - p)}{\sum_{i=1}^{n} \sum_{j=1}^{m} \eta_i \cdot r_{ij}} \\
&= \Delta LCM(p^+|p).
\end{aligned}
$$

□

A2 Data Collection

We obtained detailed operational records from a public transit agency in California, covering the actual daily mileage of 93 transit buses for the entire year of 2022. These records capture scheduled duty cycles, deviations thereof, and out-of-service movements. Since some vehicles appear to be used only for testing and training and thus have little or no mileage on most days, we excluded them from the analysis. From the remaining fleet, we selected 50 vehicles that capture the distribution of regular operational profiles in the data to improve the clarity of our results. We then calculated the energy demand r_{ij} of route i on day j by multiplying the daily mileage of each bus by an estimate of the annual average energy consumption per mile of fully battery-electric transit buses operating in California. The resulting energy demand matrix is provided in the Supplementary Data.

We complemented the route data with cost and operational parameters derived from expert interviews, technical reports, and peer-reviewed academic studies. In particular, we estimated the input parameters v^e, v^d, v, w^e, w^d, w, and θ based on a comprehensive review of recent heavy-duty road vehicle operations in the US. The estimation approach for each parameter is outlined below. Details are provided in the Supplementary Data.

We calculated the capacity-related costs of electric drivetrains, v^e, as the sum of the prices for battery packs and electric motors. Salvage values at the end of the useful lifetime of both

components were assumed to be negligible (Bach et al., 2025). To estimate the price for battery packs, we first conducted a comprehensive review of recent prices for battery packs per kWh used in commercially available heavy-duty road vehicles. Prices in currencies other than $US were converted based on the annual average exchange rate of the respective year. We also adjusted prices from before the year 2024 for inflation using the yearly inflation adjustment factor for qualified energy resources published by the US Internal Revenue Service. We then calculated the average of the adjusted prices (in $/kWh) and divided the average by a factor accounting for the practical maximum depth of discharge.

To estimate the price for electric motors per kWh, we first conducted comprehensive reviews of (i) recent prices for electric motors per kW used in commercially available heavy-duty road vehicles, (ii) their typical capacity sizes (in kW), and (iii) corresponding capacity sizes of battery packs (in kWh). We again converted prices in currencies other than $US and adjusted those from before 2024 for inflation. We then calculated the average of these prices (in $/kW), multiplied this average by the typical motor capacity (in kW), and divided the resulting value by the typical battery capacity (in kWh).

Following a similar approach, we estimated the capacity-related costs of diesel drivetrains, v^d, as the sum of the prices for diesel tanks and diesel engines. Salvage values at the end of the useful lifetime of both components were again assumed to be negligible. To estimate the prices for diesel tanks, we first reviewed recent prices for diesel tanks per gallon used in commercially available heavy-duty road vehicles, converted them to $US and adjusted them for inflation if necessary, calculated the average of these prices (in $/gallon), and divided this average by the energy density of diesel (in kWh/gallon). We then multiplied the resulting value (in $/kWh) by an adjustment factor that captures the lower energy efficiency of diesel drivetrains relative to electric drivetrains.

To estimate the price for diesel engines per kWh, we first reviewed (i) recent prices for diesel engines per kW used in commercially available heavy-duty road vehicles, (ii) their typical capacity sizes (in kW), and (iii) corresponding capacity sizes of diesel tanks (in kWh). We again converted prices to $US and adjusted them for inflation if necessary. We then calculated the average of these prices (in $/kW), multiplied this average by the typical engine capacity (in kW), and divided the resulting value by the typical size of diesel tanks (in kWh). In contrast to the diesel tank, we did not adjust the cost of the diesel engine for the lower energy efficiency, as this inefficiency mainly affects the energy required for a route

rather than the rate at which energy is delivered.

We calculated the capacity-related costs of buses, v, in several steps. First, we reviewed recent purchase prices of diesel, plug-in hybrid, and battery-electric buses. As before, we converted prices to $US and adjusted them for inflation where necessary. We then estimated the capacity-related costs of the drivetrain(s) for each of these buses based on our earlier estimates, subtracted these costs from the purchase price, and calculated the average across all residual values. We then added the discounted value of annual fixed operating expenditures for insurance, registration, and general maintenance. We again assumed no salvage value at the end of the useful lifetime.

Regarding variable operating costs, we set w^e and w^d to the 2024 annual average prices of electricity (in $/kWh) and diesel (in $/gallon) for transit agencies in California as published by the US Energy Information Administration. We then divided w^d by the energy density of diesel (in kWh/gallon) and multiplied it by the energy-efficiency adjustment factor specified above. Any variable operating expenditures for maintenance are captured by w and calculated based on a comprehensive review of recent variable maintenance costs of diesel and battery-electric transit bus operations in the US. Our calculations excluded the salary of drivers since it is the same across drivetrains.

Finally, we calculated the emission intensity of diesel drivetrains, θ, using recent data from the US Environmental Protection Agency. This report provides the amounts of individual greenhouse gases emitted by the mobile combustion of diesel fuel separately in different units. We therefore first divided the reported kilogram (kg) of carbon dioxide (CO_2) emitted per gallon of diesel combusted by the energy density of diesel (in kWh/gallon). We further multiplied the reported amounts (in kg) of methane (CH_4) and nitrous oxide (N_2O) per mile by the annual average fuel economy of diesel drivetrains in our data (in miles/gallon) and by the reported global warming potential of the respective gas. We then added these values to the amount of CO_2 emitted per kWh to obtain the overall emission intensity (in CO_2e/kWh). Finally, we multiplied this value by the energy-efficiency adjustment factor described above.

A3 Additional Analysis

Variation in Input Parameters

Our analysis has relied on point estimates for the capacity-related and variable operating costs of vehicles and drivetrains. Since the capacity sizing of drivetrains in our model depends

on relative cost differences, even small deviations in the point estimates may change the cost-efficient configuration of vehicles and the resulting total abatement cost. To examine this possibility, we repeat our calculations 50 times, each time examining a different combination of random variations between -5% and +5% in the cost variables v^e, v^d, v, w^e, w^d, and w. Positive variations for a drivetrain make it relatively less attractive to include in a vehicle.

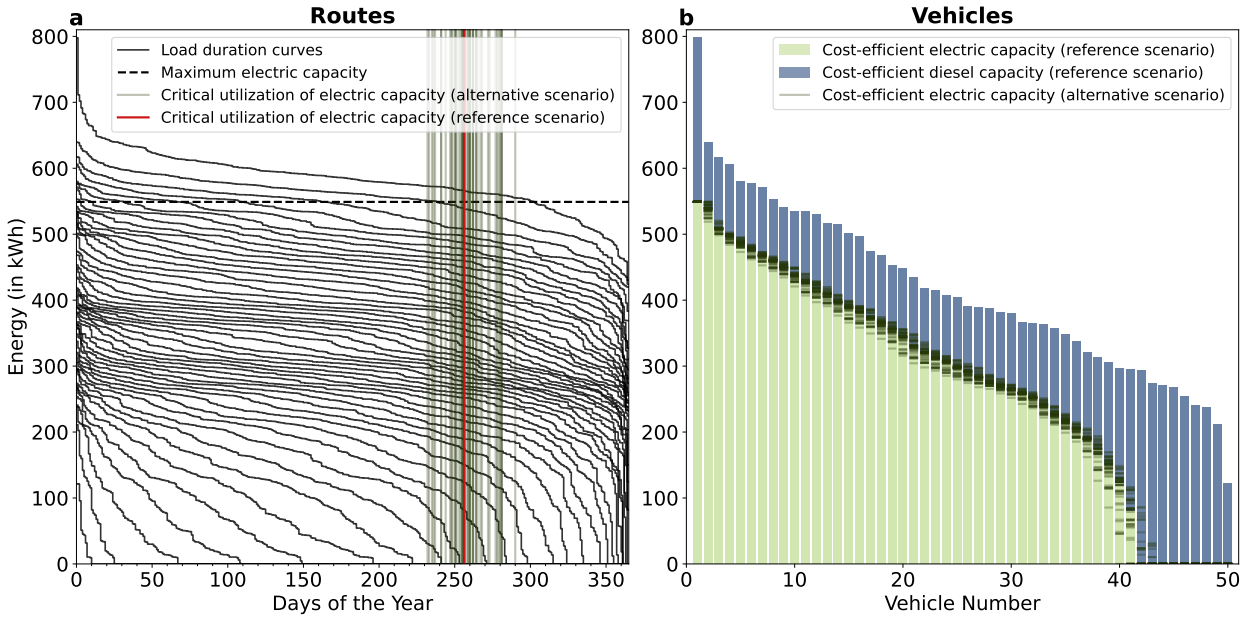


Figure A1. Cost-efficient urban bus fleet. This figure shows (**a**) the load duration curves of buses in the fleet and (**b**) the cost-efficient capacity of the electric and diesel drivetrains of the buses, assuming small simultaneous deviations in the costs of vehicles and drivetrains. The cost-efficient diesel capacity of a bus is the difference between the upper end of its blue bar and the dark green lines.

Figure A1 shows the resulting cost-efficient bus fleets across scenarios as semi-transparent dark green lines. Darker shades indicate overlapping scenarios and thus the distribution across scenarios. We find that the critical utilization of the electric capacity is moderately sensitive to the changes in cost parameters, with a standard deviation of ±5.4% relative to the reference scenario. Yet, for most buses, the cost-efficient electric and diesel capacity remain close to those in the reference scenario. This reflects that the variations in the critical utilization of the electric capacity occur in a region where the load duration curves of most buses exhibit relatively low slopes.

Figure A2 shows the corresponding total and marginal abatement cost curves as semi-transparent dark green lines. We find that the annual emissions of the cost-efficient fleet, E_0, are fairly sensitive to the changes in cost parameters, with a standard deviation of ±14.6%

relative to the reference scenario. This reflects that the small changes in the electric and diesel capacity across vehicles result in substantial changes in the total energy each drivetrain capacity delivers per year. As a consequence, the marginal abatement cost curves diverge substantially at higher emission levels. As emission targets become more ambitious, however, the costs of abatement increasingly dominate the changes in cost parameters, and the marginal abatement cost curves converge toward the reference scenario. Since the marginal abatement costs at higher emission levels are small, the total abatement cost curves across all scenarios are relatively close to the reference scenario.

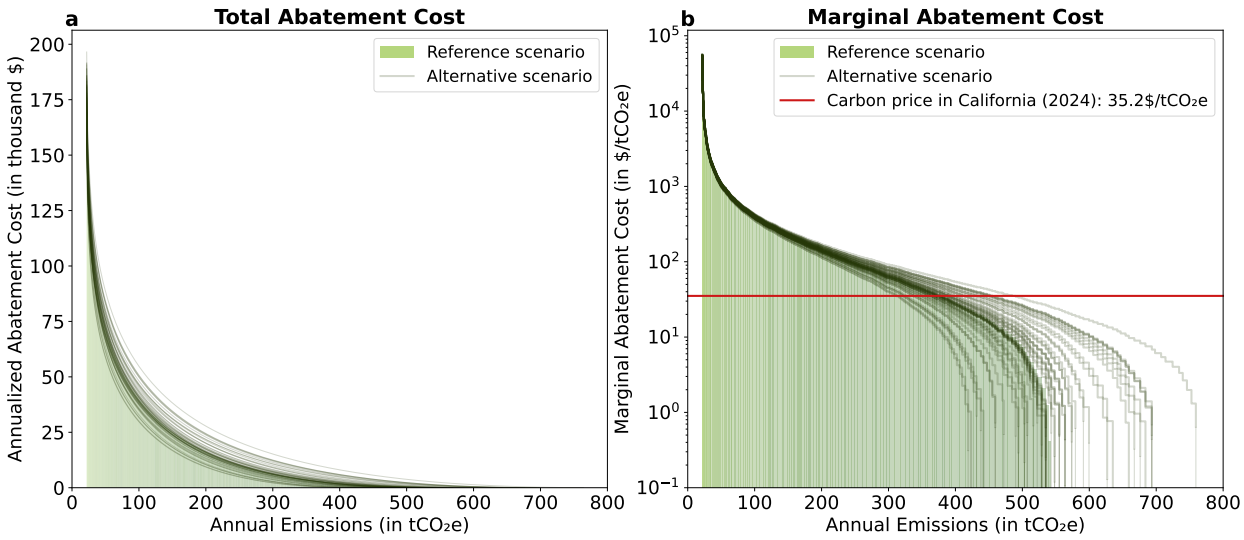


Figure A2. Abatement cost curves for urban buses. This figure shows (**a**) the annualized total abatement cost and (**b**) the marginal abatement cost for the urban bus fleet, assuming small simultaneous deviations in the costs of vehicles and drivetrains.

Advances in Battery Technology

With the adoption of electric drivetrains gaining momentum, battery technology is widely expected to improve in cost and energy density as learning effects continue to materialize with the increasing cumulative deployment. In particular, recent estimates suggest that the prices for battery packs are likely to decline by about 30–40% relative to current levels by 2030 (Link et al., 2024). To examine the impact of such advances, we calculate several scenarios where the prices for battery packs and the maximum battery capacity both improve by 10%, 20%, or 30%.

Figure A3 shows the resulting cost-efficient bus fleet across scenarios as colored lines. As battery technology improves, this fleet consists of more plug-in hybrid buses, where each bus

is equipped with a larger electric capacity than in the reference scenario. For example, with an improvement by 20%, the cost-efficient fleet consists of 44 plug-in hybrid, 6 diesel, and no fully electric buses. For the hybrid buses, the cost-efficient electric capacity ranges between 25–578 kWh (9–87% of the total energy capacity of the vehicles), with an average of 340 kWh (74%). In addition, the fleet now has a total electric capacity of 14,948 kWh (72% of the total energy capacity) and serves 5,080 MWh (93% of the total energy demand) annually using that capacity. Relative to the reference scenario, the total electric capacity and the total energy supplied by electric drivetrains are now 8.3% and 5.6% higher, respectively.

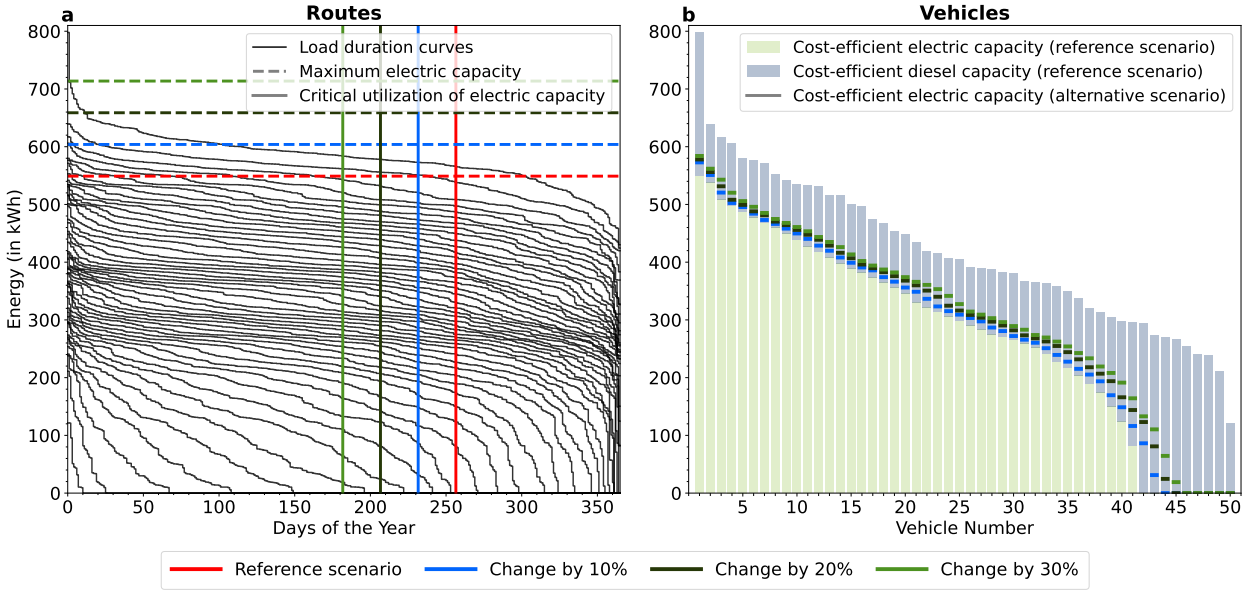


Figure A3. Cost-efficient urban bus fleet. This figure shows (**a**) the load duration curves of buses in the fleet and (**b**) the cost-efficient capacity of the electric and diesel drivetrains of the buses across alternative improvements in battery technology. The cost-efficient diesel capacity of each vehicle is given by the difference between the upper end of the blue bar and the colored line of a particular scenario.

Figure A4 shows the corresponding total and marginal abatement cost curves. Both curves retain their general shape but shift to the left as battery technology improves. The total abatement cost curve also shifts slightly downward. To calibrate, with an improvement by 20%, the annual emissions of the cost-efficient fleet amount to $E_0 = 324$ tCO_2e, and the lowest attainable emissions amount to $E_{-} = 0.3$ tCO_2e (0.1% of E_0). These values are about 40% and 99% lower than in the reference scenario, respectively. At E_{-}, all buses in the fleet are fully electric, except for vehicle 1. The corresponding annualized total abatement cost amounts to \$135,783, which is about 23% lower than the annualized total abatement cost at

$E_{-} = 21.95$ tCO_2e in the reference scenario. Alternatively, the optimal emission response to the 2024 average carbon price in California is now 242 tCO_2e (75% of E_0), which is about 36% lower than in the reference scenario.

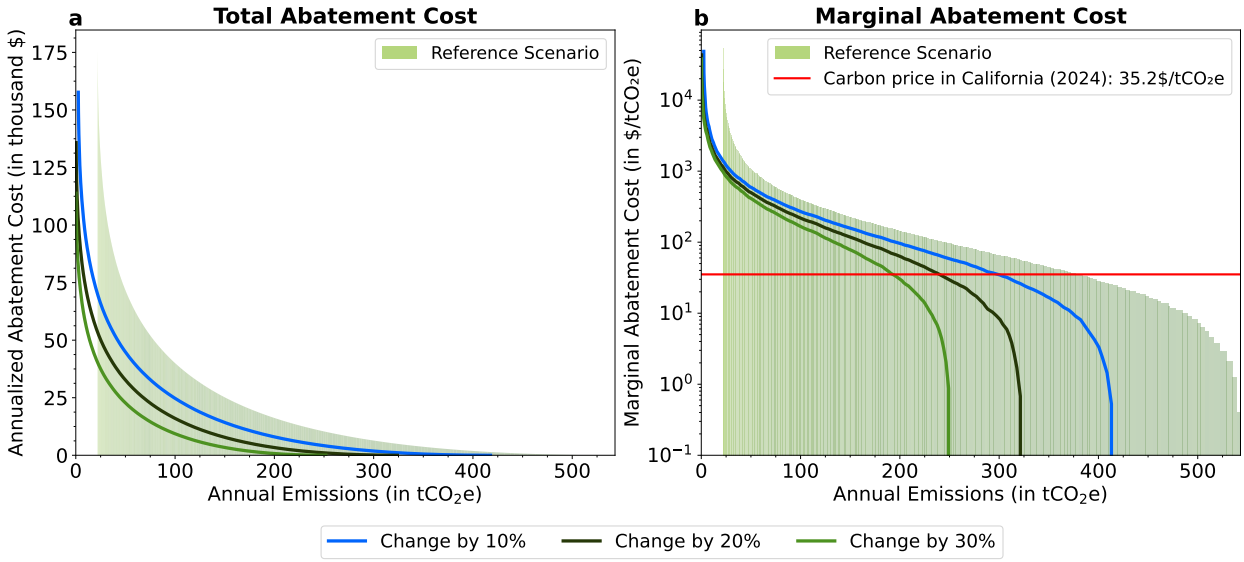


Figure A4. Abatement cost curves for urban buses. This figure shows (**a**) the annualized total abatement cost and (**b**) the marginal abatement cost for the urban bus fleet across alternative improvements in battery technology.

Low-Emission Fuels

In recent policy debates, some voices have argued that vehicles with internal combustion engines could achieve lower life-cycle net emissions by using synthetic, bio-based, or other low-emission fuels. Although the combustion of such fuels still causes direct emissions, the CO_2 emitted is argued to have been previously captured. Industry analysts estimate that switching from conventional diesel to pure biodiesel raises fuel prices by roughly 30% on an energy-equivalent basis due to the lower energy efficiency of biodiesel (U.S. Department of Energy, 2025b). Because biodiesel is typically blended with conventional diesel, we repeat our calculations for blend levels of 20%, 30%, and 40%, assuming that changes in net emission intensity and variable operating costs scale in proportion to the blend share, consistent with U.S. Department of Energy (2025a).

Figure A5 shows the resulting cost-efficient bus fleets across scenarios as colored lines. Because of the higher variable operating costs of diesel drivetrains, the critical utilization of the electric capacity shifts toward the left, and the cost-efficient fleet consists of more plug-in hybrid buses, each equipped with a larger electric capacity than in the reference scenario. For

example, with a 30% biodiesel blend, the cost-efficient fleet consists of 44 plug-in hybrid, six diesel, and no fully electric buses. For the hybrid buses, the cost-efficient electric capacity ranges between 9–549 kWh (3–86% of the total energy capacity of the vehicles), with an average of 332 kWh (72%). We also find that the fleet now has a total electric capacity of 14,614 kWh (70% of the total energy capacity) and serves 5,007 MWh (91% of the total energy demand) annually using that capacity. Relative to the reference scenario, the total electric capacity and the total energy supplied by electric drivetrains are now 6% and 4% higher, respectively.

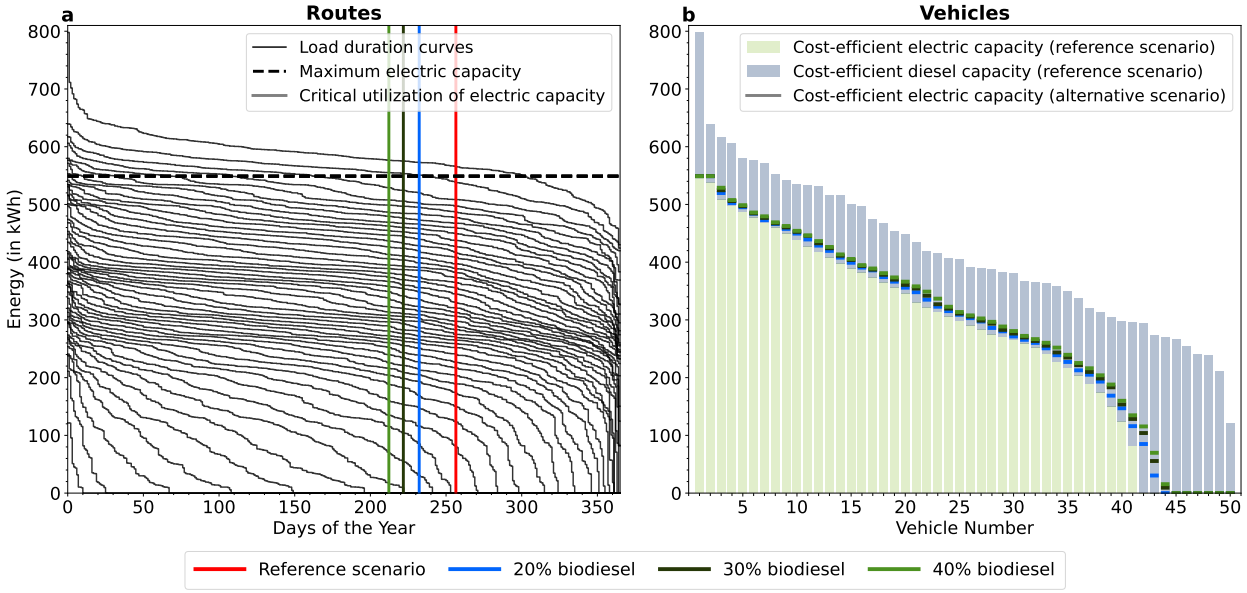


Figure A5. Cost-efficient urban bus fleet. This figure shows (**a**) the load duration curves of buses in the fleet and (**b**) the cost-efficient capacity of the electric and diesel drivetrains of the buses across alternative blend levels for biodiesel. The cost-efficient diesel capacity of each vehicle is given by the difference between the upper end of the blue bar and the colored line of a particular scenario.

Figure A6 shows the corresponding total and marginal abatement cost curves. Both curves are substantially compressed to the left as biodiesel is added to the blend. This reflects that the cost-efficient fleet now relies more on electric drivetrains and exhibits lower net emissions from using diesel drivetrains. As emission targets become more ambitious, however, the costs of electric drivetrains increasingly dominate, and the cost curves converge toward those in the reference scenario. With a 30% biodiesel blend, for example, the annual net emissions of the cost-efficient fleet amount to $E_0 = 268$ tCO_2e, which is about 51% lower than in the reference scenario. About 58% of this reduction stems from higher fuel

prices incentivizing greater electrification, while the remainder reflects the fuel's lower net emission intensity. Reducing net emissions by more than 90% to less than 26.8 tCO_2e entails annualized abatement costs of more than \$74,883, which is about 39% lower than in the reference scenario for the same absolute emission target. Alternatively, the optimal net emission response to the 2024 average carbon price in California is now 223 tCO_2e (83% of E_0), which is about 41% lower than in the reference scenario. Since the marginal abatement cost curve is compressed, the optimal net emission response to carbon prices is even less elastic than in the reference scenario.

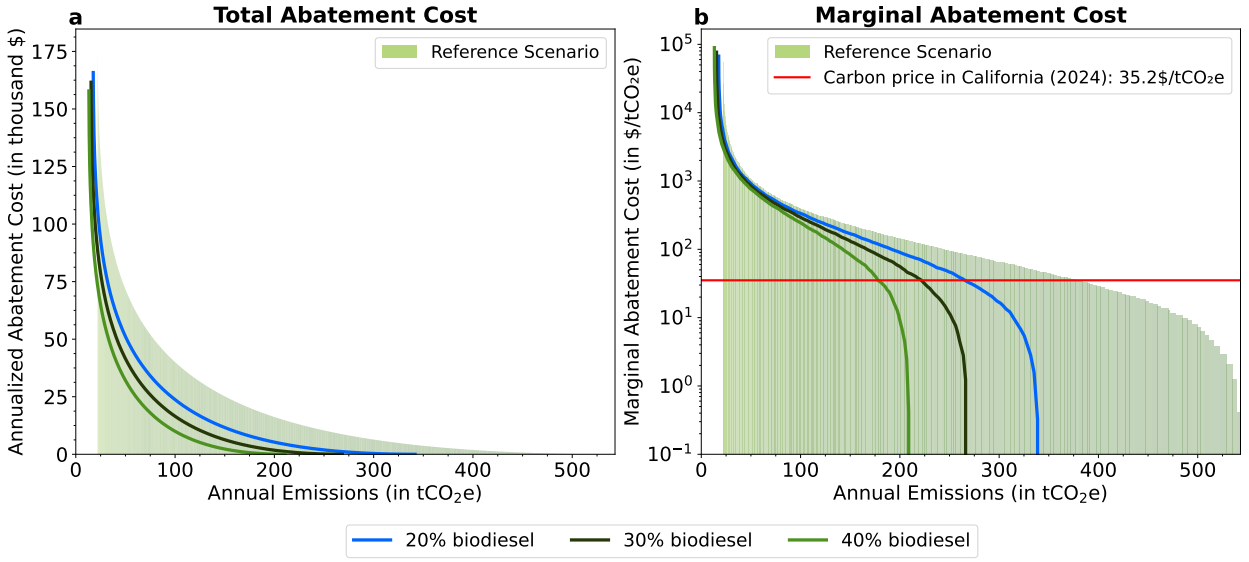


Figure A6. Abatement cost curves for urban buses. This figure shows (**a**) the annualized total abatement cost and (**b**) the marginal abatement cost for the urban bus fleet across alternative blend levels for biodiesel.

Vehicle-to-Route Assignment

Our analysis has also assumed that firms have full flexibility in assigning vehicles to routes. In practice, firms may face operational constraints to this assignment due to factors such as specific route characteristics, fixed maintenance schedules, driver scheduling and training, depot locations and infrastructure, or regulatory restrictions on vehicle types in certain zones. To examine the impact of such constraints, we repeat our numerical analysis for the extreme case where each bus on each day remains assigned to the original route observed in the operational data obtained from the public transit agency.

Figure A7a shows the resulting load duration curves of all buses in the fleet. Compared with the curves in Figure 2a, these curves intersect, form two distinct clusters, and exhibit

a wider distribution of energy demand with longer tails. This reflects that about half of the buses in the sample are diesel buses with similar drivetrain capacity, while the remaining buses have plug-in hybrid, battery-electric, or fuel-cell electric drivetrains. Consistent with Lemma 1, a cost-efficient deployment of the diesel buses on routes is then indifferent, and the firm from which we obtained the data may have aimed to use the buses evenly. In contrast to Lemma 1, the diesel buses are predominantly assigned to routes with higher energy demand, even though the other buses had sufficient energy capacity to serve most of them.

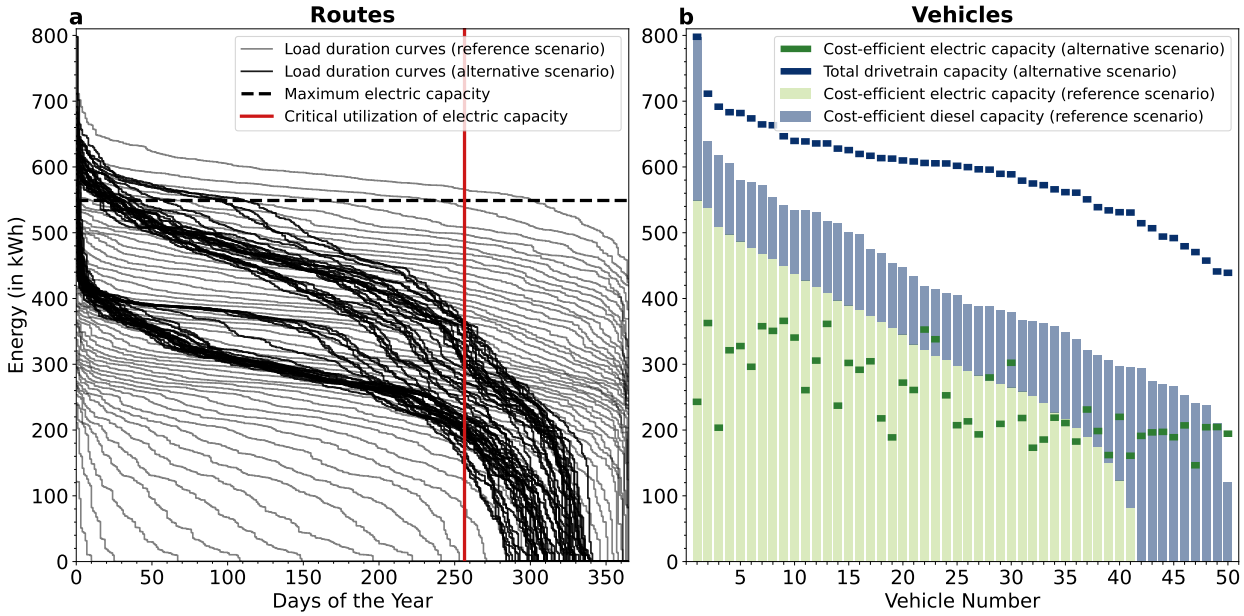


Figure A7. Cost-efficient urban bus fleet. This figure shows (**a**) the load duration curves of buses in the fleet and (**b**) the cost-efficient capacity of the electric and diesel drivetrains of the buses, assuming no reassignment of vehicles to routes. The cost-efficient diesel capacity of each vehicle is given by the difference between the dark blue line and the dark green line.

Given these load duration curves, Figure A7b shows the resulting cost-efficient configuration of buses if the firm were to acquire a new fleet. We find that this fleet now consists only of plug-in hybrid buses. The electric capacity sizes now range between 146–366 kWh (29–58% of the total energy capacity of the vehicles), with an average of 248 kWh (42%). We also find that the fleet now has a total electric capacity of 12,413 kWh (42% of the total energy capacity) and serves 3,708 MWh (68% of the total energy demand) annually using that capacity. Overall, we find that the total energy capacity of the vehicles is now 42% higher than in the reference scenario, while the total electric capacity and the total energy supplied by electric drivetrains are 10% and 23% lower, respectively.

Figure A8a shows the total abatement cost of reducing the annual emissions of the fleet from E_0 to a target level E. The annual emissions of the cost-efficient fleet now amount to $E_0 = 1,448$ tCO_2e, which is about 2.7 times higher than in the reference scenario and results directly from the significantly lower use of electric drivetrains. At the same time, the lowest attainable emission level of $E_- = 21.95$ tCO_2e remains unchanged since the number of days with energy demand greater than the maximum feasible electric capacity of 549 kWh remains unchanged. Yet, at E_-, 37 buses now have hybrid drivetrains (compared to 8 in the reference scenario) because 29 additional routes now have an energy demand peak above 549 kWh. Overall, the total abatement costs are now consistently and substantially higher than in the reference scenario, mainly because of the higher total energy capacity of the vehicles. For example, a reduction of more than 90% to less than 145 tCO_2e entails annualized abatement costs of more than \$96,972, which is about 3.7 times higher than in the reference scenario for the same absolute emission target.

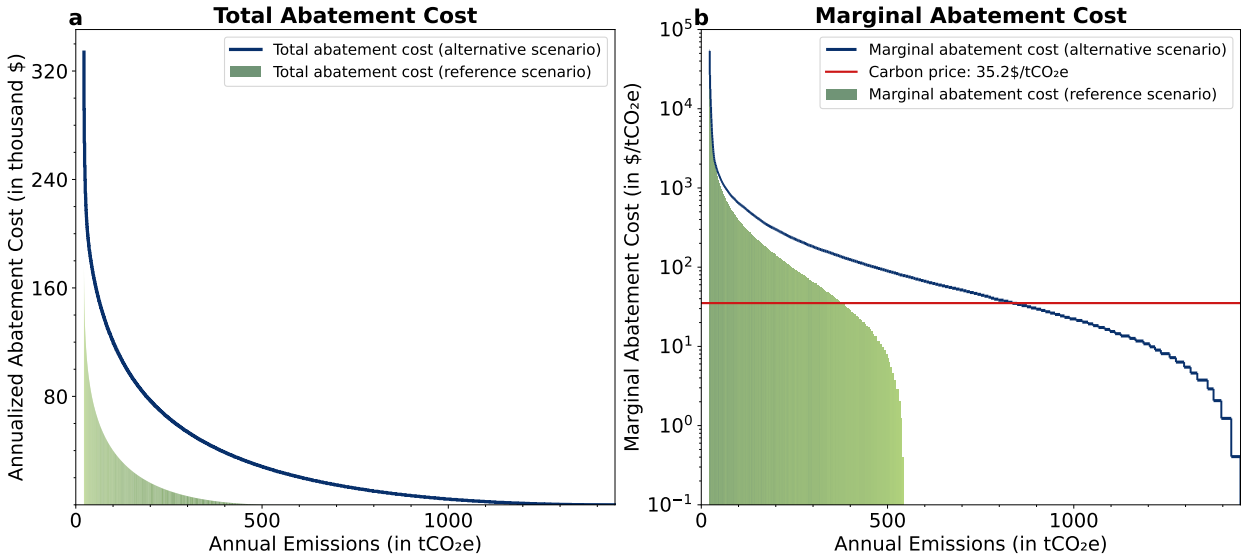


Figure A8. Abatement cost curves for urban buses. This figure shows (**a**) the annualized total abatement cost and (**b**) the marginal abatement cost for the urban bus fleet, assuming no reassignment of vehicles to routes.

Figure A8b shows the corresponding marginal abatement cost curve. While it retains its rotated S-shape when displayed on a logarithmic scale, marginal abatement costs at any emission level are substantially higher due to the lower utilization of incremental electric capacity. For example, the marginal abatement cost at $E = 500$ tCO_2e is now \$ 89.5/tCO_2e, which is about 12 times higher than in the reference scenario. Consequently, the optimal

emission response to the 2024 average carbon price in California is now 835 tCO_2e (58% of E_0), about 2.2 times the level in the reference scenario. The retained shape of the curve implies that the optimal emission response to emission charges remains fairly inelastic.

A4 Model Extensions

Our total cost of ownership model in Section 2.1 lends itself to several immediate extensions. First, in contrast to the approach above, the variables c_i^e and c_i^d can be reinterpreted as the capacity sizes of the energy component of the electric and diesel drivetrains, respectively. In addition, the firm can include fixed costs for the power component of the electric and diesel drivetrains when they are installed. The firm should then compare a vehicle's total cost of ownership, adjusted by the respective fixed costs, for three configurations: (i) a pure diesel drivetrain, (ii) a fully electric drivetrain if feasible (i.e., $\bar{c}_i^e > \max_j \{r_{ij}\}$), and (iii) a hybrid drivetrain with the electric capacity determined as in Proposition 1. The configuration with the lowest adjusted total cost of ownership identifies the cost-efficient energy capacity for the electric and diesel drivetrains of the vehicle.

Second, to capture degradation of the battery, we can specify demand across $m = 365 \cdot T$ days and reset $q_{ijk}^e = \min\{r_{ij}, \gamma_j \cdot c_i^e\}$ where γ_j denotes the share of the initial battery capacity that is still available on day j. The marginal cost of ownership for vehicle i then becomes $MCO_i(c_i^e) = (v_i^e - v_i^d) - (w^d - w^e) \cdot I_i(c_i^e)$, where the redefined $I_i(c_i^e) \equiv \sum_{j=1}^m \gamma_j \cdot \left(1 + \frac{\delta}{365}\right)^{-j} \cdot \mathbb{1}\{r_{ij} \geq \gamma_j \cdot c_i^e\}$ captures the degradation-adjusted discounted number of days over the planning horizon with energy demand $\tilde{r}_{ij} \equiv \frac{r_{ij}}{\gamma_j} \geq c_i^e$. Solving for $I_i(\cdot)$ at $MCO_i(\cdot) = 0$ yields the redefined critical utilization of the electric capacity $\lambda_i \equiv \frac{v_i^e - v_i^d}{w^d - w^e}$. Denoting by $\tilde{r}_i^u$ the u-th largest entry in the vector $(\tilde{r}_{i1}, \ldots, \tilde{r}_{im})$ and substituting it for r_i^u in Proposition 1 then identifies the cost-efficient electric capacity of vehicle i.

Third, the firm may already operate a legacy fleet of n pure diesel vehicles that can remain in service for another T years.[1] Suppose this fleet has been configured via an analogous optimization as described above, restricted to diesel drivetrains. Accordingly, each legacy vehicle i serves route i and has a drivetrain capacity of $c_i^d = \max_j \{r_{ij}\}$. Let $\rho_i \in [0, 1]$ denote the salvage value of legacy vehicle i at date $t = 0$ as a share of its initial capacity-related costs. The total cost of ownership for legacy vehicle i is then given by the opportunity cost

[1] If legacy vehicles remain operable for fewer than T years, new vehicles can be assumed to retain a salvage value equal to their fair market value at that time (Bach et al., 2025; Dutta and Reichelstein, 2021).

of retaining instead of selling the vehicle and the total variable costs of serving demand:

$$TCO_i \equiv \rho_i \cdot \left(v_i + \max_j \{r_{ij}\} \cdot v_i^d\right) + A(\delta, T) \cdot (w + w^d) \cdot \sum_{j=1}^{m} r_{ij}.$$

For each route i, the firm will replace the legacy vehicle if $TCO_i(c_i^{e*}) < TCO_i$, that is, if:

$$c_i^{e*} \cdot (v_i^e - v_i^d) - A(\delta, T) \cdot (w^d - w^e) \cdot \sum_{j=1}^{m} \min\{r_{ij}, c_i^{e*}\} > (1 - \rho_i) \cdot \left(v_i + \max_j \{r_{ij}\} \cdot v_i^d\right),$$

where c_i^{e*} is determined as in Proposition 1. If $\rho_i = 1$, the right-hand side equals zero, and the firm's decision coincides with the base model above. Yet, if $\rho_i \in [0, 1)$, then the variable costs savings from adopting the new vehicle with electric drivetrain must also offset the unrecovered portion $(1 - \rho_i)$ of the legacy vehicle's capacity-related costs to justify replacement.

A5 Alternative Model Applications

In this section, we argue that our model is applicable to other vehicle fleets and to other industries with multiple operating assets. Urban delivery vans, municipal refuse trucks, regional delivery trucks, and port drayage trucks operate on regular duty cycles and return to central depots overnight (Bruchon et al., 2024). Compared with urban buses, their utilization across vehicles tends to be more uniform, as they lack the pronounced morning and evening peaks associated with passenger travel. Their load duration curves are characterized by many days with similar energy demand, occasional moderate peaks (e.g., during holidays or severe weather), and regular downtime on weekends. If the critical utilization of electric capacity is sufficiently low, the cost-efficient electric capacity likely constitutes most, if not all, of the required total energy capacity of a vehicle. Accordingly, electric light-commercial vehicles have recently experienced exponential sales growth worldwide (IEA, 2025b).

Ride-hailing and other passenger vehicles can usually be fully replenished overnight. Yet, they may not return to central depots, and their daily duty cycles are often stochastic. As noted in Section 2.1, fleet operators will then seek to assign vehicles to routes based on the cumulative energy demand across days between depot returns. They will further seek to determine the cost-efficient electric capacity based on the expected number of days with sufficiently high energy demand. The load duration curves of such vehicles are typically

characterized by many days with relatively low energy demand and a substantial number of days with pronounced peaks driven by elevated passenger travel or long-distance trips (Plötz et al., 2017). As a consequence, the cost-efficient configuration of such vehicles tends to combine an electric drivetrain sized to cover most days with lower energy demand with a conventional drivetrain to meet occasional peak demand. This configuration reflects the setup of most plug-in hybrid passenger vehicles sold today (IEA, 2025b).

Long-haul trucks operate on regular, high-mileage duty cycles but may not return to home depots for several days. While conventional drivetrains can typically be fully refueled daily, battery-electric drivetrains often cannot yet be fully recharged daily due to limited charging infrastructure at distribution centers and along highways. The load duration curves of long-haul trucks exhibit consistently high energy demand on most days, a few exceptional peaks driven by heavy loads or energy-intensive routes, and regular downtime on weekends and holidays (Hunter et al., 2021). Such technological and economic constraints corroborate the observation that long-haul truck sales have remained dominated by conventional drivetrains (IEA, 2025b). Yet, rapid advances in battery technology, continuous expansion of fast-charging infrastructure, and the arrival of new truck models with electric drivetrains suggest that this pattern is likely to change over the coming years.

Shipping contributes about 2% of global annual CO_2 emissions (IEA, 2025c), with nearly all originating from the combustion of oil in deep-sea cargo vessels, including container, bulk, and tanker ships. Container ships typically follow regular duty cycles, calling at multiple ports over several days or weeks, while bulk and tanker ships operate more opportunistically between individual ports. Their load duration curves exhibit, on most days, consistently high energy demand from propulsion at sea and, on remaining days, low energy demand from auxiliary systems while in port. To curb emissions, shipping companies seek to adopt low-emission fuels such as ammonia, biofuels, hydrogen, and methanol (IMO, 2025). They also seek to electrify auxiliary systems via onboard batteries and shore-power connections at ports. In contrast to cargo ships, regional ferries tend to operate on fixed schedules with moderate energy demand and daily returns to berth. Such conditions have facilitated the early adoption of vessels with battery-electric propulsion by operators in Norway (Nkesah and Solvoll, 2022).

Aviation accounts for about 2.5% of global annual CO_2 emissions (IEA, 2025a), with almost all coming from the burning of kerosene in commercial airplanes. Most commercial

airplanes operate multi-leg rotations spanning several flights over one or more days. Their load duration curves are shaped by sustained high energy demand from propulsion during flight and minimal energy demand from auxiliary systems while on the ground. To reduce emissions, airlines primarily seek to increase the share of sustainable aviation fuel produced from biomass or electrolytic hydrogen combined with CO_2. Ground operations tend to draw power from airport grids already. Meanwhile, aircraft manufacturers are developing new propulsion systems, including hydrogen combustion turbines and electric propulsion via batteries, hydrogen fuel cells, or hybrid-electric configuration combining conventional and electric systems (IEA, 2025a).

Beyond the transportation sector, technology firms typically serve a global time-variant energy demand for computing power with data centers located around the world. To power these data centers, they can either draw electricity from the local grids and incur the embodied emissions or install renewable energy and storage systems (see, for instance, Apple (2024); Google (2025); Microsoft (2025)). Analysts can adapt our model to determine the cost-efficient renewable energy capacity at each data center based on its load duration curve and the local and temporal availability of wind and solar resources. They can further use our model to assess the costs of expanding renewable energy capacity across data centers to meet firm-wide emission targets.

Similarly, companies with multiple offices, retail sites, or production facilities face local energy needs for electricity, heating, and cooling. At present, electricity is usually sourced from local grids, while heat is typically generated by onsite natural gas boilers. Firms can decarbonize their operations by investing in renewable energy sources to substitute grid electricity and by installing heat pumps to replace gas boilers (see, for instance, Aldi (2025); Lidl (2022)). Heat pumps eliminate direct emissions, yet they increase electricity demand and may raise overall emissions depending on the emission intensity of the local grids. Analysts can adapt our model to coordinate investments in renewable power and heat pumps across locations based on local variations in grid emissions and the cost of wind and solar power.

References

Catrina Achilles, Peter Limbach, Michael Wolff, and Aaron Yoon. Inside the Blackbox of Firm Environmental Efforts: Evidence from Emissions Reduction Initiatives. 2025. URL `https://dx.doi.org/10.2139/ssrn.4856016`.

Aldi. Climate, 2025. URL https://bit.ly/4nM2boQ.

Apple. Apple ramps up investment in clean energy and water around the world. 2025-11-10, 2024. URL https://bit.ly/43lz58v.

Anthony Atkinson, Robert Kaplan, Ella Matsumura, and Mark Young. *Management Accounting: Information for Decision Making*. Cambridge Business Publishers, Cambridge, 7 edition, 2020.

Alessandro Avenali, Giuseppe Catalano, Mirko Giagnorio, and Giorgio Matteucci. Assessing cost-effectiveness of alternative bus technologies: Evidence from US transit agencies. *Transportation Research Part D: Transport and Environment*, 117(October 2022):103648, 2023.

José Azar, Miguel Duro, Igor Kadach, and Gaizka Ormazabal. The Big Three and corporate carbon emissions around the world. *Journal of Financial Economics*, 142(2):674–696, 2021.

Amadeus Bach, Simona Onori, Stefan Reichelstein, and Jihan Zhuang. Fair Market Value of Used Capacity Assets: Forecasts for Repurposed Electric Vehicle Batteries. *The Accounting Review*, 2025.

Jennie Bai and Hong Ru. Carbon Emissions Trading and Environmental Protection: International Evidence. *Management Science*, 70(7), 2024.

Ramji Balakrishnan and K. Sivaramakrishnan. A Critical Overview of the Use of Full Cost Data for Planning and Pricing. *Journal of Management Accounting Research*, 14(1):3–31, 2002.

Tim Baldenius, Sunil Dutta, and Stefan Reichelstein. Cost allocation for capital budgeting decisions. *The Accounting Review*, 82(4):837–867, 2007. ISSN 00014826.

Rajiv D. Banker and John S. Hughes. Product Costing and Pricing. *The Accounting Review*, 69 (3):479–494, 1994.

Nicola J. Beaumont and Robert Tinch. Abatement cost curves: A viable management tool for enabling the achievement of win-win waste reduction strategies? *Journal of Environmental Management*, 71(3):207–215, 2004.

Tobias Berg, Lin Ma, and Daniel Streitz. Out of sight, out of mind: Divestments and the Global Reallocation of Pollutive Assets. *Journal of Financial Economics*, 182(104308), 2026. URL https://doi.org/10.1016/j.jfineco.2026.104308.

BNEF. Electric Vehicle Outlook 2025, 2025. URL https://about.bnef.com/electric-vehicle-outlook/.

Patrick Bolton and Marcin T. Kacperczyk. Firm Commitments. *Management Science*, 0(0):1–34, 2025.

Matthew Bruchon, Brennan Borlaug, Bo Liu, Tim Jonas, Jiayun Sun, Nhat Le, and Eric Wood. Depot-Based Vehicle Data for National Analysis of Medium- and Heavy-Duty Electric Vehicle Charging, 2024. URL `https://docs.nrel.gov/docs/fy24osti/88241.pdf`.

Rainer Burkard, Mauro Dell'Amico, and Silvano Martello. *Assignment problems*. Society for Industrial and Applied Mathematics, Philadelphia, 2009.

Rainer E. Burkard, Bettina Klinz, and Rüdiger Rudolf. Perspectives of Monge properties in optimization. *Discrete Applied Mathematics*, 70(2):95–161, 1996.

CARB. California transitioning to all-electric public bus fleet by 2040, 2018. URL `https://bit.ly/4s0Sy8W`.

Shira Cohen, Igor Kadach, Gaizka Ormazabal, and Stefan Reichelstein. Executive Compensation Tied to ESG Performance: International Evidence. *Journal of Accounting Research*, 61(3):805–853, 2023.

Jonathan Colmer, Ralf Martin, Mirabelle Muûls, and Ulrich J. Wagner. Does Pricing Carbon Mitigate Climate Change? Firm-Level Evidence from the European Union Emissions Trading System. *Review of Economic Studies*, 92(3):1625–1660, 2025.

Stephen Comello, Gunther Glenk, and Stefan Reichelstein. Transitioning to clean energy transportation services: Life-cycle cost analysis for vehicle fleets. *Applied Energy*, 285(March):116408, 2021.

Stephen Comello, Julia Reichelstein, and Stefan Reichelstein. Corporate Carbon Reduction Pledges: An Effective Tool to Mitigate Climate Change? In *Frontiers in Social Innovation*. Harvard Business Review Press, Boston, 2022.

Hemang Desai, Pauline Lam, Bin Li, and Shiva Rajgopal. An Analysis of Carbon-Reduction Pledges of U.S. Oil and Gas Companies. *Management Science*, 69(6):3748–3758, 2023.

Benedikt Downar, Jürgen Ernstberger, Stefan Reichelstein, Sebastian Schwenen, and Aleksandar Zaklan. The impact of carbon disclosure mandates on emissions and financial operating performance. *Review of Accounting Studies*, 26:1137–1175, 2021.

David F. Drake. Carbon tariffs: Effects in settings with technology choice and foreign production cost advantage. *Manufacturing and Service Operations Management*, 20(4):667–686, 2018.

David F. Drake, Paul R. Kleindorfer, and Luk N. Van Wassenhove. Technology choice and capacity portfolios under emissions regulation. *Production and Operations Management*, 25(6):1006–1025, 2016.

Sunil Dutta and Stefan Reichelstein. Decentralized capacity management and internal pricing. *Review of Accounting Studies*, 15(3):442–478, 2010.

Sunil Dutta and Stefan Reichelstein. Capacity rights and full-cost transfer pricing. *Management Science*, 67(2):1303–1325, 2021.

Alexander Dyck, Karl V. Lins, Lukas Roth, and Hannes F. Wagner. Do institutional investors drive corporate social responsibility? International evidence. *Journal of Financial Economics*, 131(3): 693–714, 2019.

Alexander Dyck, Karl V. Lins, Lukas Roth, Mitch Towner, and Hannes F. Wagner. Renewable Governance: Good for the Environment? *Journal of Accounting Research*, 61(1):279–327, 2023.

Paolo Falbo, Giorgio Ferrari, Giorgio Rizzini, and Maren Diane Schmeck. Optimal switch from a fossil-fueled to an electric vehicle. *Decisions in Economics and Finance*, 44(2):1147–1178, 2021.

Gunther Glenk and Stefan Reichelstein. The Economic Dynamics of Competing Power Generation Sources. *Renewable and Sustainable Energy Reviews*, 168(112758):1–9, 2022.

Gunther Glenk, Rebecca Meier, and Stefan Reichelstein. Constructing Carbon Abatement Cost Curves. *The Accounting Review*, 101(3):223–255, 2026.

Google. Driving sustainable innovation for society, 2025. URL `https://datacenters.google/operating-sustainably`.

Robert F. Göx. Capacity Planning and Pricing under Uncertainty. *Journal of Management Accounting Research*, 14(1):59–78, 2002.

Michael Grubb, Jean Charles Hourcade, and Karsten Neuhoff. *Planetary Economics: Energy, Climate Change and the Three Domains of Sustainable Development.* Routledge, New York, 2014.

Tubagus Aryandi Gunawan and Rory F.D. Monaghan. Techno-econo-environmental comparisons of zero- and low-emission heavy-duty trucks. *Applied Energy*, 308:118327, 2022.

Andrew Harris, Danielle Soban, Beatrice M. Smyth, and Robert Best. A probabilistic fleet analysis for energy consumption, life cycle cost and greenhouse gas emissions modelling of bus technologies. *Applied Energy*, 261:114422, 2020.

Charles Horngren, Srikant Datar, and Madhav Rajan. *Cost Accounting - A Managerial Emphasis.* Pearson, Boston, 15 edition, 2015.

Shanshan Hu, Gilvan C. Souza, Mark E. Ferguson, and Wenbin Wang. Capacity Investment in Renewable Energy Technology with Supply Intermittency: Data Granularity Matters! *Manufacturing & Service Operations Management*, 17(4):480–494, 2015.

Chad Hunter, Michael Penev, Evan Reznicek, Jason Lustbader, Alicia Birky, and Chen Zhang. Spatial and Temporal Analysis of the Total Cost of Ownership for Class 8 Tractors and Class 4 Parcel Delivery Trucks, 2021. URL `https://www.nrel.gov/docs/fy21osti/71796.pdf`.

ICAP. California Cap-and-Trade Program, 2025. URL `https://bit.ly/3WMRV4L`.

IEA. Aviation, 2025a. URL `https://bit.ly/3JUQWMU`.

IEA. Global EV Outlook 2025, 2025b. URL `https://bit.ly/3JWghWI`.

IEA. International Shipping, 2025c. URL `https://bit.ly/3Lz0cXB`.

IMO. IMO's work to cut GHG emissions from ships, 2025. URL `http://bit.ly/4oFrTwc`.

Ioannis Ioannou, Shelley Xin Li, and George Serafeim. The effect of target difficulty on target completion: The case of reducing carbon emissions. *The Accounting Review*, 91(5):1467–1492, 2016.

IPCC. Summary for Policymakers. In *Climate Change 2023: Synthesis Report. Contribution of Working Groups I, II and III to the Sixth Assessment Report of the Intergovernmental Panel on Climate Change*, pages 1–34. IPCC, Geneva, 2023.

Özge Islegen and Stefan Reichelstein. Carbon Capture by Fossil Fuel Power Plants: An Economic Analysis. *Management Science*, 57(January):21–39, 2011.

Martin Jacob and Kira Lena Zerwer. Emission Taxes and Capital Investments: The Role of Tax Incidence. *The Accounting Review*, 99(5):247–278, 2024.

Mark Jacobsen and Arthur van Benthem. Vehicle Scrappage and Gasoline Policy. *American Economic Review*, 105(3):1312–1338, 2015.

Xiaoyan Jiang, Shawn Kim, and Shirley Lu. Limited accountability and awareness of corporate emissions target outcomes. *Nature Climate Change*, 15(March), 2025.

Paul L Joskow. Comparing the costs of intermittent and dispatchable electricity generating technologies. *American Economic Review*, 101(3):238–241, 2011.

Gürhan Kök, Kevin Shang, and Şafak Yücel. Investments in renewable and conventional energy: The role of operational flexibility. *Manufacturing and Service Operations Management*, 22(5): 925–941, 2020.

Kathryn Kynett. The California Cap-and-Trade Program: Overview and Considerations for Congress, 2024. URL https://www.congress.gov/crs-product/R48314.

Eva Labro. Costing Systems. *Foundations and Trends in Accounting*, 13(3-4):267–404, 2019.

Antti Lajunen and Timothy Lipman. Lifecycle cost assessment and carbon dioxide emissions of diesel, natural gas, hybrid electric, fuel cell hybrid and electric transit buses. *Energy*, 106(2016): 329–342, 2016.

Lidl. 100 Prozent Grünstrom, 5.000 Photovoltaikanlagen: Die Schwarz Gruppe macht sich stark für den Klimaschutz, 2022. URL https://bit.ly/3LoRfA7.

Steffen Link, Annegret Stephan, Daniel Speth, and Patrick Plötz. Rapidly declining costs of truck batteries and fuel cells enable large-scale road freight electrification. *Nature Energy*, 9(8):1032–1039, 2024.

McKinsey. A cost curve for greenhouse gas reduction, 2007. URL http://bit.ly/3kpYxWA.

Microsoft. Our 2025 Environmental Sustainability Report, 2025. URL https://bit.ly/3XiP2sr.

Hee Seung Moon, Won Young Park, Thomas Hendrickson, Amol Phadke, and Natalie Popovich. Exploring the cost and emissions impacts, feasibility and scalability of battery electric ships. *Nature Energy*, 10(1):41–54, 2025.

Sergey Naumov, David R Keith, and John D Sterman. Accelerating vehicle fleet turnover to achieve sustainable mobility goals. *Journal of Operations Management*, 69(1):36–66, 2023.

Stephen Nkesah and Gisle Solvoll. Implementing zero emission vessels in ferry operations in Norway. *Proceedings from the Annual Transport Conference at Aalborg University*, 29:1–15, 2022.

Bessie Noll, Santiago del Val, Tobias S. Schmidt, and Bjarne Steffen. Analyzing the competitiveness of low-carbon drive-technologies in road-freight: A total cost of ownership analysis in Europe. *Applied Energy*, 306:118079, 2022.

Shyam S.G. Perumal, Richard M. Lusby, and Jesper Larsen. Electric bus planning & scheduling: A review of related problems and methodologies. *European Journal of Operational Research*, 301 (2):395–413, 2022.

Patrick Plötz, Niklas Jakobsson, and Frances Sprei. On the distribution of individual daily driving distances. *Transportation Research Part B: Methodological*, 101:213–227, 2017.

Stefan Reichelstein and Anna Rohlfing-Bastian. Levelized Product Cost: Concept and decision relevance. *The Accounting Review*, 90(4):1653–1682, 2015.

Ralph Tyrrell Rockafellar. *Convex Analysis*. Number 28. Princeton University Press, Princeton, NJ, 1997.

Lingling Shi, Suresh P. Sethi, and Metin Çakanyıldırım. Promoting electric vehicles: Reducing charging inconvenience and price via station and consumer subsidies. *Production and Operations Management*, 31(12):4333–4350, 2022.

Robert N. Stavins. *Economics of the Environment: Selected Readings*. Edward Elgar Publishing, Inc., Northampton, MA, 7 edition, 2019.

Annika Stechemesser, Nicolas Koch, Ebba Mark, Elina Dilger, Patrick Klösel, Laura Menicacci, Daniel Nachtigall, Felix Pretis, Nolan Ritter, Moritz Schwarz, Helena Vossen, and Anna Wenzel. Climate policies that achieved major emission reductions: Global evidence from two decades. *Science*, 385(6711):884–892, 2024.

Boris Stolz, Maximilian Held, Gil Georges, and Konstantinos Boulouchos. Techno-economic analysis of renewable fuels for ships carrying bulk cargo in Europe. *Nature Energy*, 7(2):203–212, 2022.

The European Commission. ETS 2: Buildings, road transport and additional sectors, 2025. URL `https://bit.ly/4a5XsdR`.

Christopher Timmins, Roger H. von Haefen, and Shanjun Li. How Do Gasoline Prices Affect Fleet Fuel Economy? *American Economic Journal: Economic Policy*, 1(2):113–137, 2009.

Sorabh Tomar. Greenhouse Gas Disclosure and Emissions Benchmarking. *Journal of Accounting Research*, 61(2):451–492, 2023.

U.S. Department of Energy. Biodiesel Blends, 2025a. URL `https://afdc.energy.gov/fuels/biodiesel-blends`.

U.S. Department of Energy. Clean Cities and Communities Alternative Fuel Price Report, 2025b. URL `https://bit.ly/3Zt7pfr`.

Wenbin Wang, Mark E. Ferguson, Shanshan Hu, and Gilvan C. Souza. Dynamic capacity investment with two competing technologies. *Manufacturing and Service Operations Management*, 15(4): 616–629, 2013.

Maxwell Woody, Gregory A. Keoleian, and Parth Vaishnav. Decarbonization potential of electrifying 50% of U.S. light-duty vehicle sales by 2030. *Nature Communications*, 14(1):1–12, 2023.

Contact.

MIT CEEPR Working Paper Series
is published by the MIT Center for Energy and Environmental Policy Research from submissions by affiliated researchers.
For inquiries and/or for permission to reproduce material in this working paper, please contact:

General inquiries: ceepr@mit.edu
Media inquiries: ceepr-media@mit.edu

Copyright © 2026
Massachusetts Institute of Technology



MIT CEEPR

Center for Energy and
Environmental Policy Research

MIT Center for Energy and
Environmental Policy Research
Massachusetts Institute of Technology
77 Massachusetts Avenue, E19-411
Cambridge, MA 02139-4307
USA

ceepr.mit.edu

MASSACHUSETTS INSTITUTE OF TECHNOLOGY